SOUTHERN ILLINOIS PALEOCLIMATE DETERMINED FROM VARIATIONS IN IRON OXIDE CONTENT

by

JAMES L. BLANKENSHIP

Presented to the Faculty of the Graduate School of

The University of Texas at Arlington in Partial Fulfillment

of the Requirements

for the Degree of

MASTER OF SCIENCE IN GEOLOGY

THE UNIVERSITY OF TEXAS AT ARLINGTON

May 2008

ACKNOWLEDGEMENTS

I would like to thank Dr. William Balsam, my supervising professor, for his patience, guidance, and willingness not to give up on me during this project even though at times I wanted to give up on myself. Additionally, very special thanks to the instructors and staff at the UTA Geology Department, most notably Dr. Merlynd Nestell and his wife Galina for their guidance and support. I would also like to thank Dr. Charles Onasch and Dr. John Farver of Bowling Green State University for seeing the potential in me to do graduate work and the encouragement to stick with it.

A number of people have been instrumental in my graduate and professional career, most notably, my best friend Bryan Gibbs who has supplied me with endless nights of conversation pertaining to the betterment of my graduate work. In addition, I would like to thank the staff at SMMS laboratory for working around my schedule throughout the project and encouraging me along the way. The Russ Martin Show on 105.3 FM deserve a very special thanks for providing me a place to hang out with my buddies a few hours a week and forget the world, even if it is just for a few hours its meant more to me than you know, thank you. To all of my family and friends that have helped me through this, thank you very much, your assistance and support are much appreciated.

None of this would have been possible without the support and patience from my wife Michelle who has stood by me with unwavering stamina. Most of all, I would

like to extend a heartfelt expression of gratitude to my grandparents, Charles and Maxine Allen, for their irreplaceable wisdom and teachings that have allowed me to excel this far in life.

April 28, 2008

ABSTRACT

SOUTHERN ILLINOIS PALEOCLIMATE
DETERMINED FROM VARIATIONS
IN IRON OXIDE CONTENT

James L. Blankenship, M.S.

The University of Texas at Arlington, 2008

Supervising Professor: Dr. Merlynd Nestell

Diffuse reflectance spectroscopy was used to determine the relative abundance of the iron oxides hematite and goethite in a loess and paleosol sequence from an unglaciated area of southern Illinois. Factor analysis of first derivatives of the spectral data yielded a four factor solution which explained more than 94% of the cumulative variance. Factors 2 and 3, which represent hematite and goethite respectively, were the most useful for interpreting paleoclimatic conditions at the site. Hematite, which is indicative of warmer conditions with periodic seasonal rainfall, shows a strong response not only to climatic variations but also to glacial lobe proximity. Goethite is generally associated with loess where conditions favored a cooler and moister environment and exhibits a strong correlation to glacial intervals with the exception of the Roxana loess,

where large amounts of quartz and secondary carbonate interfere with the signal. Together, factor 2 (hematite) and factor 3 (goethite) illustrate a paleoclimatic record of southern Illinois for the last 11 glacial/interglacial episodes.

TABLE OF CONTENTS

LIST OF ILLUSTRATIONS

LIST OF TABLES

CHAPTER 1

INTRODUCTION

The study of loess and paleosols has gained importance during the last century because of their relationship to climatic change. Paleosols form during interglacial conditions whereas loess is indicative of glacial conditions. The Chinese loess sequence, the best known and most highly studied loess, contains the longest continuous terrestrial record of climate change known, extending back at least 2 million years (Kukla, 1987). In North America loess sequences are not as long, but are still significant because they record climate change as a result of glacial advance and retreat for the last several hundred thousand years. Loess is generally considered to be a wind blown silt (2 to 64 μm) deposit derived from either peri-glacial grinding of rock debris that is subsequently deposited on flood plains or from a desert origin (Pye, 1995a). It is usually tan to yellow in color and appears as a thick (1m or more) homogenous layer in outcrop. Interbedded with the loess are paleosols that formed during periods that were warmer (Kemp, 2001). Paleosols can range in color from brown to red and generally contain evidence of root casts, bioturbation, and pedogenesis.

The majority of research on loess has been undertaken on the Chinese loess sequence in Northern China, where the loess/paleosol sequence may be up to 300 m in thickness, and it is commonly referred to in the literature as the Chinese Loess Plateau

(CLP). Studies of Chinese loess (Ji et al., 2001, 2004; Maher et al., 2003; Balsam et al., 2004, 2005) have shown fairly precise correlations of iron oxides to average rainfall and glacial to interglacial scale climate change. The concentrations of iron oxides, especially goethite and hematite, have been shown to correspond to loess formation and paleosol development in the CLP (Ji et al., 2001; Balsam et. al, 2004). Other research has correlated the Chinese Loess sequence to global marine records showing a global climate oscillation between glacial and interglacial cycles throughout the Quaternary (Liu and Ding, 1998; Kukla and An, 1989; Helsop et al., 2000; Porter, 2001). These large scale comparisons are made possible by examining the oxygen isotope ratios (O^{18}:O^{16}) from foraminifers in marine cores (Lowe and Walker, 1997). Isotopically light O^{16} is preferentially removed from the oceans during glacial periods through evaporation and incorporation into the continental ice/glacier. It is subsequently released as meltwater during interglacials distorting the ratio in the opposite direction (Lowe and Walker, 1997). By examining this oscillation between the two isotopes, a generalized curve can be constructed to show glacial/stadial and interglacial/interstadial events over time on a global scale (Johnsen et al., 1995; Lowe and Walker, 1997). These alternating stages are numbered sequentially from the present day backwards through time where odd numbers reflect interglacial conditions (present day is Stage 1) and even numbers denote glacial conditions. They may also be subdivided into smaller units which are intended to denote oscillations between dominant climate regimes (ex. stage 5a-5e) (Reading, 1996; Lowe and Walker, 1997).

Unlike the CLP, North American loess/paleosol research has been limited to small geographic regions even though loess deposits cover a large area throughout the Mid-West from Nebraska to Mississippi (Figure 1). At least in part, this compartmentalization of loess research in North America results from somewhat tenuous correlations to global events suggesting that loess sequences reflect primarily local conditions and secondarily global events. Workers in these local regions have developed their own stratigraphy and there is little or no stratigraphic continuity from one region to another across the Mid-West. Whereas stratigraphic correlations have been proposed (Follmer, 1996), these loose connections fall short of addressing the larger picture of loess and paleosol deposition in North America and its relation to past global climate. Forman and Pierson (2002) published a luminescence chronology for a portion of the North American loess record and related this chronology to input of glacial melt water to the Gulf of Mexico. Grimley et al. (1998) and Mason (1998) have shown climatic variations recorded in the Peoria Loess through a variety of methods including organic content, carbonate content, and magnetic susceptibility combined with mineral zonations. They use these data to illustrate their model of ice sheet movement during the last glaciation. Other studies of loess on the North American continent are generally regional (ex. Nebraska, Illinois, Alaska) and focus on a relatively short time scale from the last glacial interval to a few hundred thousand years (Muhs and Bettis, 2000, Muhs et al., 2003; O'Geen and Busacca, 2001; Mason, 2001; Davis, 2002; Blinnikov, 2002).

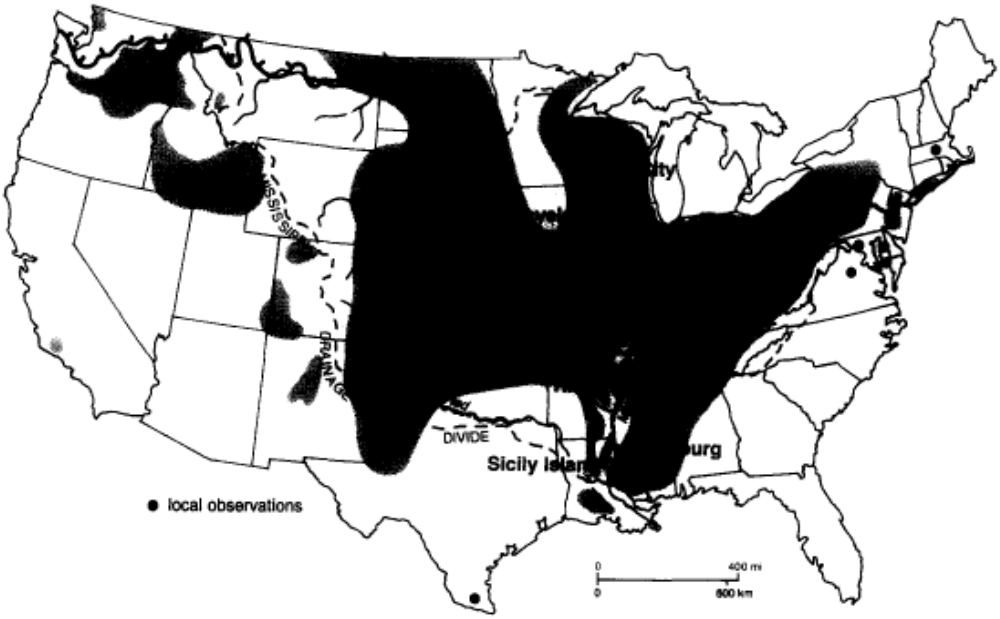

Figure 1. The Peoria Loess (Wisconsian in age) blankets a large portion of the United States and is considered to be the most continuous loess deposit at or near the surface (after Follmer, 1996).

Although many different indicators of climate have been applied to the North American loess sequence, none is particularly direct. This study uses a more direct indicator of climate, iron oxide mineralogy. The iron oxide mineral hematite (αFe_2O_3) and oxyhydroxide mineral goethite ($\alpha FeO(OH)$) were identified by their visible light (VIS) reflectance spectrum. Hematite formation, which is partial to a drier and warmer environment, will show higher values for interglacial and interstadial periods, whereas goethite formation, which is favored by cooler and moister environments, will show higher values for glacial and stadial periods. This technique was applied to an unstudied loess and paleosol sequence in a non-glaciated area of southwestern Illinois.

One of the reasons to use reflectance spectrophotometry is its ability to identify iron oxide minerals at extremely low concentrations, typically at least an order of magnitude lower than XRD (Deaton and Balsam, 1991). This characteristic of reflectance spectra has proved valuable in analyzing loess and paleosol sequences, primarily because hematite and goethite occur in low concentrations in these sediments (Balsam et al., 2004).

CHAPTER 2

PREVIOUS WORKS

2.1 General Loess Terminology and Research

Although there are references in the Chinese literature dating back over 1,000 years, the origins of loess studies are generally attributed to European scientists of the early to mid 1800's (Smalley et al., 2001). Karl Caesar Von Leonhard of Heidelberg, Germany coined the term loess c. 1820 and it is most likely a derivative of the name *"Loesch",* which was the term used by the people of the Upper Rhine area to describe the yellow lime soil *"Lischen"* or "snail shell soil" that is easily loosened (Kirchheimer in Smalley et al., 2001). Charles Lyell was responsible for putting loess on the world stage after his interaction with Leonhard in Heidelberg and with the incorporation of loess into his book *The Principles of Geology volume 3* (c. 1833) launched a new era of study into the nature, origin, and formation of loess (Smalley et al., 2001).

Loess and reworked loess comprise approximately 10% of the Earth's land surface (Reading, 1996). In general, loess is considered to be a fine grained silt deposit formed by eolian processes. Whereas loess sediment may have multiple source areas, its formation can be explained through three primary environments. The first primary environment of loess formation, which is somewhat interrelated to the second, comes from the grinding of glacial debris by an active glacier. This theory was first proposed by John Hardcastle of New Zealand in 1890 but was not popularized until Pavel

Tutkovskii published his work on this theory in 1899 (Smalley et al., 2001). As the debris is ground and reworked by the glacier, fine grained sediment or "rock flour" accumulates within the ice until melting occurs which is then transported as outwash and deposited at the glacial margin. These sediments may then be thrown into suspension and deposited several kilometers downwind of these proglacial outwash areas (Reading, 1996). Secondly, loess can be generated from river terraces and flood plains that accumulate vast amounts of unconsolidated fine grained sediment, primarily from large glacial outwash, which are easily sent aloft during dry periods and deposited downwind in areas of wind deceleration (Reading, 1996).

The third environment for loess formation is the arid or desert environment which was first proposed by Russian scientist Vladimir Afanas'evich Obruchev in 1911 (Smalley et al., 2001). Fine grains in an arid environment can be picked up and held aloft for several kilometers due to the high winds, low vegetation, frequent/large temperature fluctuations, and lack of moisture content in the region. This is evident in China, where loess on the CLP forms an extensive blanket across a majority of the country due to the large source of fine sediment from the Gobi Desert (Sun, 2002).

The discovery of paleosols interbedded in the Chinese loess opened up a new view of loess and it's relation to the Pleistocene environment (Smalley et al., 2001). It is widely accepted that these interbedded paleosols formed under warmer conditions with more frequent seasonal rainfall than the loess. Several studies, more than are mentioned here, (Kukla, 1987; Ji et al., 2001, 2002, 2004; Chen et al., 2002; Balsam et al., 2004, 2005) have compared the alternating loess and paleosol beds of the Chinese

Loess Plateau to glacial and interglacial intervals, where the glacial intervals support the dry, cold air needed for transport and deposition of loess, and the interglacials provide moisture and warmth for plant growth and soil development.

2.2. North American Loess

Loess in North America was first recognized by Lyell in 1846 along the bluffs of the lower Mississippi River and was generally believed to be a fluvial deposit (Follmer, 1996; Rutledge et al., 1996; Smalley et al., 2001). This idea of a fluvial or in-situ deposit would persist and compete with the eolian theory of deposition for the next 100+ years with the publication by L.S. Berg in 1916 essentially suggesting that loess is formed where it is found (Smalley et al., 2001). Later publications promoted this contrast in ideas about loess origin and formation well into the 1950's (Follmer, 1996; Rutledge et al., 1996). Although much debate continues on the origin, formation, and definition of loess, in this work North American loess is accepted as an eolian silt deposit, primarily derived from proglacial outwash and/or flood plain aridification during glacial periods. Numerous studies of loess have been done in the United States, but most focus on a small temporal range (10,000-100,000 year) and a localized geographic area. Although these studies have proven useful for understanding loess formation at different times and in different and regions, they have also muddled what should be a laterally semi-continuous stratigraphic record of loess and paleosol in North America (Follmer, 1996). Follmer (1996), and more recently Rutter et al. (2006), have made some attempts at resolving the continuity problem, but there is not yet a consensus on the continuity of North American loess. Figure 2, from Follmer's 1996

paper, illustrates this continuity problem where it is quite obvious that research has been done in localized settings resulting in multiple names for stratigraphically equivalent units. Recent methods in dating have been used to show some correlation among units (Forman and Pierson, 2002) but more research is needed in this area.

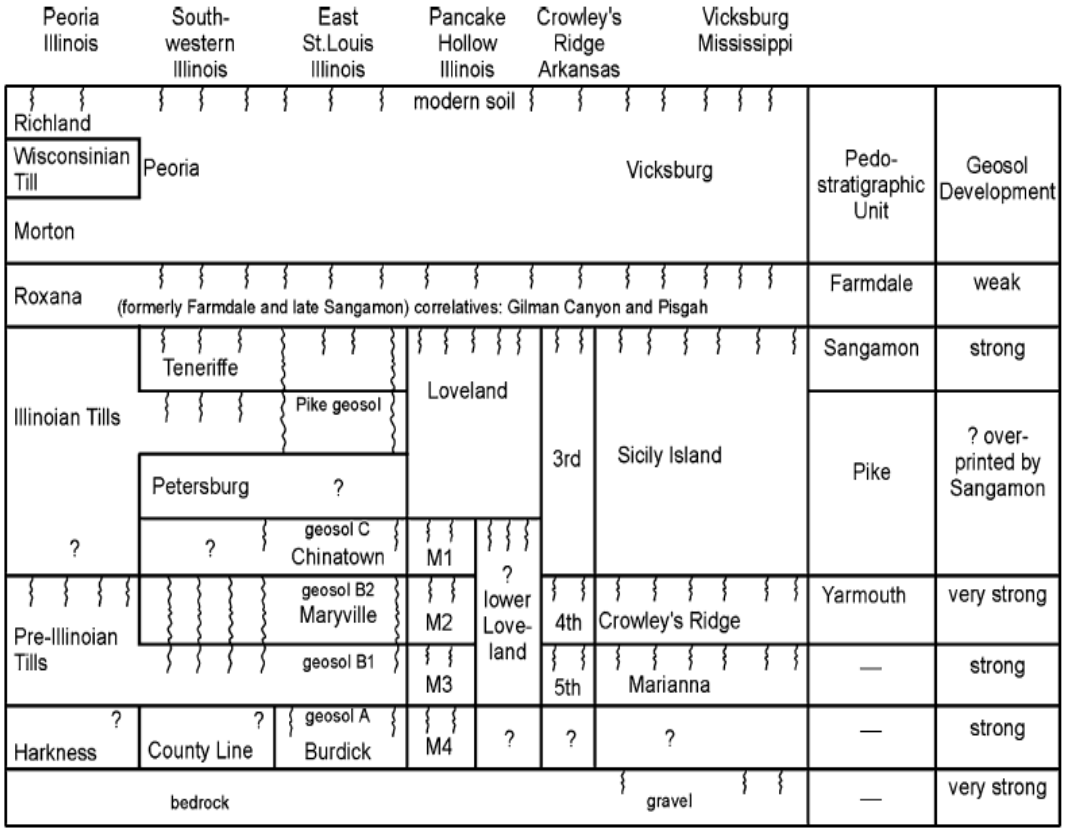

Figure 2. Correlation of loess deposits in the Lower Mississippi Valley, from Follmer (1996).

2.3 Hematite and Goethite Formation in Soils and Loess

Compared to the pale yellow goethite-rich loess, paleosols are generally higher in hematite content which is easily seen in cores or outcrops by its pronounced redness.

Soils in which hematite (and to some extent goethite) is currently forming are slightly acidic to calcareous, well aerated, permeable, and occur in warm sub-humid to arid environments where the relative humidity is less than about 40% (Schwertmann, 1971, Langmuir, 1997). The formation of hematite occurs primarily by the weathering and oxidation of Fe (especially ferrous) silicate minerals or by the aging of Ferrihydrite/hydrous ferric oxide (HFO) (Fe $(OH)_3$ nH_20), which is the initial precipitate from the rapid hydrolysis of Fe(III) or oxidation of Fe(II) (Langmuir, 1997; Costantini et al, 2006).

The most abundant oxyhydroxide in sedimentary environments is goethite and it is the most stable oxyhydroxide in cooler, moister environments (Langmuir, 1997). Hematite transforms to goethite in soils when transitioning from a warmer drier environment to a cooler moister environment, and the reason and mechanism for this transformation is a result of the changing dynamics of the organic matter in the soil regime (Schwertmann, 1971; Langmuir, 1997). As the climate becomes cooler and the moisture increases, the rate of organic matter decomposition decreases, causing an excess build up of organic compounds in the soil which dissolves the hematite through reduction and complexation of the iron. After being reprecipitated the newly formed oxide is goethite (Schwertmann, 1971). The presence of hematite and goethite is not exclusive to either loess or paleosol; rather, hematite and goethite may be present in both loess and paleosol, and their concentration is generally dictated by the environmental conditions at the site of formation (Ji et al., 2001).

2.4 NUV/VIS/NIR Reflectance

Reflectance spectroscopy is the study of the amount of light reflected or scattered from a surface at a given wavelength (Clark, 1995). The human eye is a crude recorder of reflected light. It takes in red, green and blue wavelengths of light and combines them into an overall perceived color or hue. However, in reflectance spectrophotometry light reflected from a sample is recorded progressively as percent reflectance versus wavelength for the spectral range of the instrument; frequently data can be recorded at intervals as small as 1 nm.

The ability to distinguish slight spectral differences is of great advantage to anyone doing research on mineral mixtures where it is difficult to discern low concentrations of significant minerals in sediments. This capacity to show slight compositional changes is intrinsic to the method of reflectance where light is reflected, scattered, and absorbed (Clark, 1995). In a mixture of light and dark grains, for example quartz and magnetite, the lighter grains will tend to have high reflectance values indicating that many of the photons are being scattered or reflected whereas the darker grains will absorb photons at nearly every photon-grain interaction, accounting for reduced reflectance even though their weight percentage to light grains is very small. As a general rule, darker grains will dominate the reflectance spectra in mixtures (Clark, 1995). This inherent process of absorption, scattering, and reflectance has proven useful for studying loess and paleosols because two of the climatically important minerals in loess and paleosols, hematite and goethite, are present in extremely low concentrations, frequently less than 1% by weight (Clark, 1995; Balsam and Deaton,

1991, 1996; Balsam and Wolhart, 1993; Balsam et al., 1995; Balsam and Beeson, 2003; Balsam et al., 2004, 2005,).

2.5 NUV/VIS/NIR Reflectance Applied to Loess Studies

A majority of loess studies involving reflectance spectrophotometry is from the Chinese Loess Plateau (Balsam et al., 2004; Chen et al., 2002; Ji, et al., 2001, 2002, 2004). Ji's 2002 study demonstrates that reflectance data can be used to quantitatively estimate the concentrations of iron oxides in loess and paleosol by % weight. Loess and paleosol samples were deferrated by the CBD procedure to produce a natural matrix to which known concentrations of hematite and goethite were added, thus providing a set of calibration standards. The samples were spectrally analyzed and through multiple linear regression analysis, calibration equations provided wt. % hematite and goethite with a correlation coefficient of >0.93 (Ji et al., 2002).

Other notable studies have been carried out (Balsam et al., 2004, 2005 and Ji et al., 2004) and demonstrate that reflectance data is very useful for the determination of iron oxide concentrations, and hence paleoclimate variability in the alternating loess and paleosols of the Chinese Loess Plateau. Balsam's 2004 (in Balsam et al., 2004) study using spectral data shows how changing concentrations of iron oxides in the CLP are related to precipitation variability from Asian monsoons. Using pedogenic production of hematite and magnetite to precipitation and hematite to goethite ratios Balsam (in Balsam et al., 2004) proposed a paleoclimate model including two distinct phases of precipitation.

CHAPTER 3

STUDY AREA AND CORE DESCRIPTION

The samples were provided by the Illinois State Geological Survey (ISGS) located at the University of Illinois, Urbana-Champaign. Two cores were drilled at the Simmons Farm in Monroe County, Illinois at the eastern edge of the Mississippi valley (38° 7'30"N, 90° 7'30"W) (Figure 3) (Wang, personal communication). The two cores were combined to reflect the full extent of the core, in other words, one core was used to supplement missing intervals in the other thus giving a continuous core for analyses. Dr. Hong Wang and Dr. Leon Follmer provided access to the core at ISGS, and Dr. Wang oversaw and participated in sampling of the cores.

The Simmons Core (Figure 4) contains 5 interglacial paleosols, 2 interstadial paleosols, and 5 loess units (Wang, personal communication). The five interglacial paleosols are referred to as the Modern, Sangamon, Yarmouth, Paleosol 3 and Paleosol 4 (Wang, personal communication). The two interstadial paleosols are the Chapin and Prairie Du Rocher, and the five loess units are the Peoria, Roxana, Loveland, Crowley's Ridge and the Mariana (Wang, personal communication). A portion of the core is missing, lost in extraction, and is presumed to be the well known interstadial Farmdale paleosol observed elsewhere locally as the dividing unit between the Peoria and the Roxana loess units (May and Holen, 1993).

Modern soils in southern Illinois, which are generally Alfisols, are derived from deciduous forests. These soils contain a 10 centimeter thick dark A horizon, a pale E horizon, and a reddish brown Bt horizon over 1 meter thick. A description of soil horizons and their properties are presented in Table 1. The modern soil unit has developed on the underlying Peoria Loess and is approximately 1.2 meters thick. It is distinguished from the grayish brown color of the Peoria Loess by its distinctive reddish brown Bt horizon (Wang, personal communication).

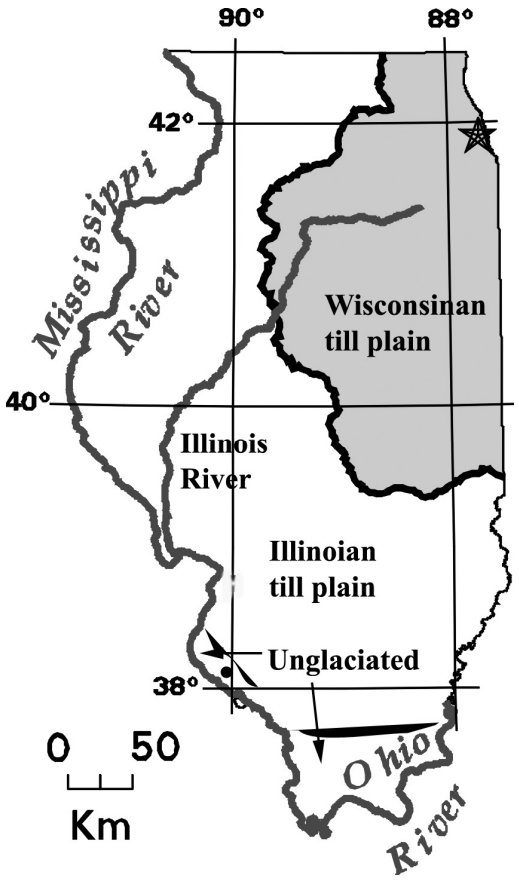

Figure 3. Location of the Simmons Core (near 38°) is in the unglaciated area of southwestern Illinois (Wang, personal communication).

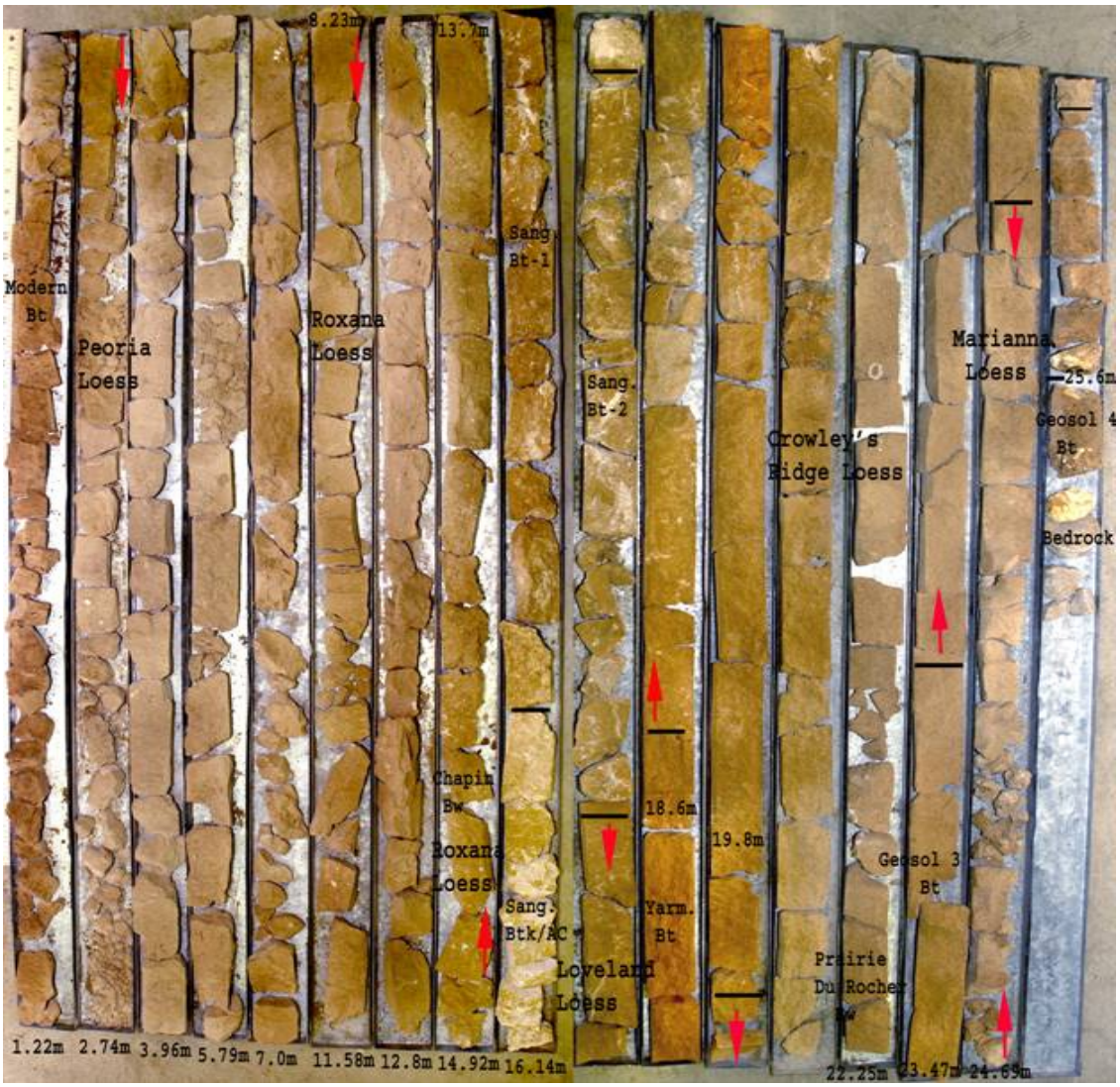

Figure 4. Complete section of the Simmons Core showing 5 interglacial paleosols, 2 interstadial paleosols, and 5 loess units. The Farmdale paleosol would be located between the Peoria and Roxana Loess (bottom of 4th tray from left to the top of the 5th tray) (Wang, personal communication).

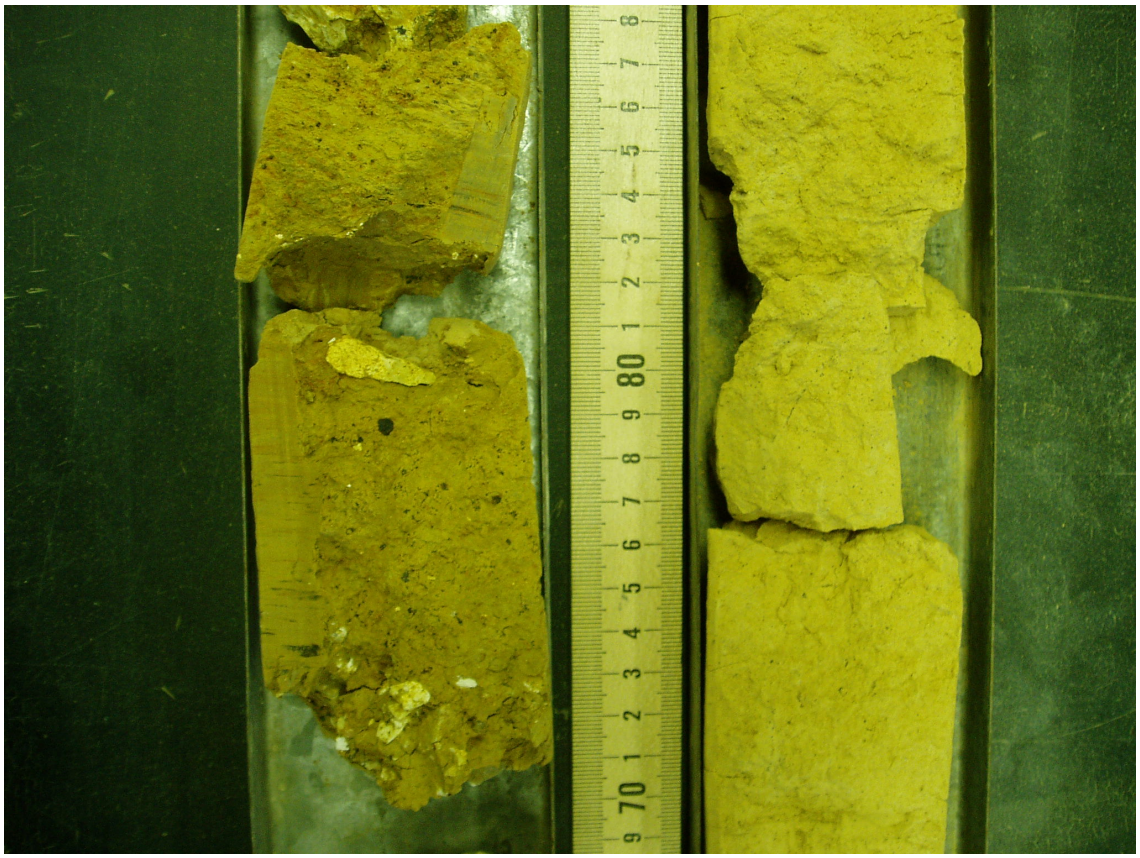

Figure 5. Representative samples of a paleosol (left) and a loess unit (right) from the Simmons core.

Table 1. Soil horizons (Modified after Lowe and Walker, 1997).

Horizon	Description
O	The O horizon consists of organic debris such as leaf litter and decomposed organic matter (humus).
A	Generally referred to as topsoil. Dark organic rich layer of humus and mineral particles. Facilitates seed germination and root growth.
AC	These horizons contain properties that are similar to the upper A horizon and the lower C horizon. They are transition zones where weathering has not distinguished this zone to be classified as a B horizon.
E	Zone of eluviation (leaching) and is pale in color. Composed primarily of sand and silt size particles due to the loss of minerals and clays through the downward percolation of ground water.
B	Also referred to as the sub-soil. Minerals and clays (iron, aluminum oxides, and carbonates) accumulate and deposit here from the above layers. A Bt horizon denotes accumulation of clay lamellae and a Bw horizon denotes a weakly developed B horizon yet still distinguishable from the horizons above and below.
C	Also known as the Regolith. This layer contains slightly broken up parent material and little to no organic content, roots do not penetrate here.
R	Generally considered bedrock and show little or no effect of weathering

The Peoria Loess was deposited in southern Illinois during the late Wisconsian glaciation between 24-25 and 10-14 ka (Pye et al., 1995b; Follmer, 1996; Forman and Pierson, 2002; Roberts et al., 2003; Wang et al., 2006). At the Simmons Farm site it has a thickness of approximately 5.5 meters and contains five weakly developed paleosol A horizons representing warmer and wetter interstadial or semi-interstadial climates (Wang, personal communication). Local pollen data suggest that the area at the time of formation was a very cold and moist environment, suitable for a boreal forest or tundra like vegetation and that precipitation exceeded or was equal to evaporation (Curry and Baker, 2000). Grain size analysis of the Peoria loess in the

Great Plains area indicate that the deposit becomes progressively finer towards the Mississippi River (west to east), indicating that it is most likely derived from ice margin sediments deposited by the Wisconsian ice sheet (Mason et al., 1994).

The Roxana Loess is pink to tan in color and 8.0 meters thick. According to thermoluminesence dating (Forman and Pierson, 2002) the basal Roxana in this area is about 55 ± 5 ka (Leigh and Knox, 1993). This unit corresponds to the early Wisconsian glaciation where climatic conditions were cold and moist, supporting an open boreal forest, yet having a high seasonality change in temperature (Curry and Baker, 2000). The Roxana can be divided into two sub units, the lower Markham and the upper Meadows members which are separated by the 0.6 meters thick interstadial Chapin Bw Geosol (Wang, personal communication). The lower Markham member is a tan colored silt unit whereas the upper Meadows member can be divided into upper pink, middle tan, and lower pink segments (Wang, personal communication).

The Sangamon paleosol underlies the Roxana Loess and is believed to have a basal age of started formation about 135 to 125 ka which coincides with the onset of the last interglacial (Curry and Pavich 1996, 2000; Jacobs 1998a, 1998b; Forman and Pierson, 2002; Grimley et al., 2003;). The Sangamon is approximately 2.3 meters thick and is widely known in the Midwest because of its thick, well expressed, reddish brown Bt horizon.

The Loveland Loess is approximately 1.3 meters in thickness and brown to tan in color. It is composed of fine grained silt that is finer than that of the Peoria and Roxana (Wang, personal communication). The Loveland is believed to coincide with

Marine Isotope Stage 6 and have a basal age of started deposition about 190 ka (Mirecki and Miller, 1993; Maat and Johnson, 1996; Forman and Pierson, 2002; Grimley et al., 2003).

The Yarmouth paleosol is extremely red in color, 1.8 meters in thickness, and is recognized as an Utisol or a soil having a subtropical origin (Wang, personal communication). The bright red color and strong soil fabric are remarkably different than the Modern soil and Sangamon Geosol, making the Yarmouth easily identified in outcrops and cores (Wang, personal communication). The Yarmouth paleosol is considered by some researchers to have been formed solely during Marine Isotope Stage 7 (Forman and Pierson, 2002; Rutter et al., 2006), whereas others have placed the formation and development from Marine Isotope Stage 7 through 11 based on weathering intensity (Grimley et al., 2003).

The fourth loess unit is stratigraphically correlated to the Crowley's Ridge Loess unit in the Lower Mississippi Valley (Grimley, et al., 2003; Wang, personal communication). It is light yellowish silt and 2.5 meters in thickness. Thermoluminesence dates from the Crowley's Ridge section in Arkansas and Iowa suggest that the onset of deposition for this unit in these areas is between 200 to 250 ka and 184 to 224 ka, respectively (Wang, personal communication; Markewich et al., 1998; Forman and Pierson, 2002). The Crowley's Ridge Loess unit contains the newly identified interstadial, named Prairie Du Rocher after the area near the core site, which is approximately 0.6 meters in thickness (Wang, personal communication).

The fourth paleosol in the core is not yet formally named or correlated with paleosols in any other area because this is the first time that it has been identified in this region; and it is simply referred to as Paleosol 3. Its Bt horizon is orange in color and consists of a silty clay. It is similar in texture and development to that the Bt horizon of the Yarmouth Paleosol.

The fifth loess is 1.2 meters in thickness and is known as the Mariana Loess in Arkansas. It has not been identified elsewhere in this region and there is no direct information about the stratigraphic contact between the Crowley's Ridge Loess and the Mariana Loess (Follmer, 1996; Wang, personal communication).

The fifth and final unit in the Simmons Core is 0.3 meters in thickness, and is referred to as Paleosol 4. The Bt horizon is a dark brown silty clay loam with Fe-Mn stains and thick clay skins. This unit rests on limestone bedrock. A complete stratigraphy of the Simmons Core (after Wang, personal communication) is shown in Table 2.

Table 2. Description of the Simmons core (after Wang, personal communication).

Stratigraphy	Depth (m)	Pedofeatures
Modern Soil	0-1.2	A: 4cm, dark, organic rich, silty loam; strong aggregated granular particles; root traces and worm channels; voids; leached. E: 6cm, pale silty loam; root traces; bio-aggregation; granular; some iron stains in matrix; leached (10YR 7/4). Bt: 1.1m, reddish silty clay loam (7.5 YR 5/4); angular blocky, prismatic structures; Fe-Mn stains, thick clay skins; leached.
Peoria Loess	1.2-6.7	AC profile: Light grayish (10YR 6/4); calcareous, fine sandy silt; massive, containing numerous reddish weathering bands, known as paleosol A horizon complexes.
Roxana Loess	6.7-14.7	AC profile: Subdivided into 4 silt units: upper pink (7.5 YR 5/5), 6.7-9.1m ; middle tan, 9.1-10.4m; lower pink, 10.4-13.4 m; and bottom tan, 13.4-14.6m; Coarse silt, fine sand, massive, some intervals leached.
Chapin Paleosol	13.4-14.0	Bw: yellowish silt loam (10 YR 6/4); prismatic structure; large voids; secondary carbonate fillings.
Sangamon Paleosol	14.7-17.0	Bt: reddish (7.5 5/4 YR); silty clay loam; angular blocky, sub-angular blocky; distinctive clay skins with Fe-Mn stains; root traces, animal burrows, voids; Upper Bt: 14.7-15.5m; Btk/AC: 15.5-16.2m; Lower Bt: 16.2-17.0m.
Loveland Loess	17.0-18.3	AC profile: brownish silt loam (10 YR 5/5); partially leached; carbonate concretions; massive.
Yarmouth Paleosol	18.3-20.1	Bt: bright reddish silty clay (5 YR 5/6); smooth rounded blocky, very thick clay skins with Fe-Mn concretions and stains; root traces, animal burrows, voids; hard when dry.
Crowley's Ridge Loess	20.1-22.6	AC profile: light yellowish silt loam (10 YR 7/6); leached; finer texture; weak aggregation.
Prairie Du Rocher Paleosol	21.3-21.9	Bw: yellowish silt loam (10 YR 8/5); subangular block; thin and sparse clay skins; carbonate rhizoliths; developed in the middle of the Crowley's Ridge Loess.
Paleosol 3	22.6-23.7	Bt: ocher silty clay (7.5 YR 6/4), smooth rounded blocky; thick clay skins; distinct Fe-Mn stains; root traces, animal burrows, voids; has a similar fabric strength to the Yarmouth Bt horizons.
Marianna Loess	23.7-24.7	AC profile: light yellow silt loam (10YR 7/4); dense, leached; coarser texture.
Paleosol 4	24.7-25.6	Bt: brown to reddish silty clay loam (5YR 4/3), subangular blocky, clay skins, Fe-Mn- stains, root traces, animal burrows, voids; highly leached; pebbles.
Bedrock	25.6-	Limestone.

CHAPTER 4

METHODS

4.1 Sample Preparation

The core was separated into individual samples at a 3 cm interval and placed into bags numbered 001 through 793 starting at the top of the core (0 meters depth). A small number of samples that were included in the partitioning of the core were omitted from the analysis (<6 overall) because they were not indicative of the loess or paleosol composition, i.e., they were composed primarily of concretions and contained little or no sediment.

The procedure used to process the samples is outlined in Balsam and Deaton (1991) and is the basis for the present study. Small amounts of each sample (1-3 grams) were placed in aluminum dishes and dried for 18-24 hours in an oven at approximately 45°C. The dried samples were then pulverized with a mortar and pestle to an average grain size of less than 38µm. Approximately 0.15 grams of the sample were placed on a pre-cleaned glass micro slide (25 x 40 mm) and suspended in 3 to 4 drops of distilled water. The slurry was then mixed and smoothed with a small metal spatula and dried overnight at 25°C. Slides produced in this manner have a smooth, uniform opaque surface necessary to obtain high quality reflectance data.

4.2 Analytical Techniques

Diffuse reflectance spectra were determined using a Perkin-Elmer Lambda 6 NUV/VIS/NIR Spectrophotometer with a diffuse reflectance attachment. This instrument has two light sources (Deuterium for UV and Tungsten for VIS/NIR wavelengths), a movable grating (to separate the light into wavelengths), and a photomultiplier tube to measure the intensity of the reflected wavelengths. The intensity of the reflected wavelengths of each sample is compared to a barium sulfate standard that establishes 100% reflectivity. Data from the samples were recorded at 1nm intervals on a floppy disk from the near ultraviolet, through the visible, and into the near infrared (250nm to 850nm). Data were analyzed from 395nm to 705nm at 10nm intervals because iron oxides show a strong and distinctive spectral response in the visible range and 10nm intervals are deemed sufficient intervals for data reduction after experimental methods showed that there is little to no difference at this interval compared to 1nm intervals (Balsam and Deaton, 1991).

4.3 Data Reduction

Reflectance spectra are a quantitative measurement of the ratio of the intensity of light reflected from the surface of a sample to the intensity of light incident upon it. The relative intensity of the light reflected is dependant upon the composition of the sample and is recorded as a percent reflectance per nanometer (Balsam and Deaton, 1991; Clark, 1995). The spectral curves for the samples of the North American loess section were reduced to a few basic mineral assemblages by factor analysis, after the methods of Balsam and Deaton (1991).

Raw reflectance curves are generally smooth and featureless making them difficult to interpret or differentiate from one another. There are, however, slight changes in the slope of a spectral curve that become prominent when the data is plotted as first derivatives of the reflectance values (Figure 6a-b). This method for analyzing spectral curves as a first derivative was used by Barranco et al. (1989) and later refined by Balsam and Deaton (1991).

In this study, first derivative curves were calculated at 10nm intervals as percent per nanometer and then plotted at the midpoint of the interval used. Figure 6a-b is an example of a spectral curve from a sediment mixture compared to its first derivative curve, which illustrates how slight changes in the spectral curve show up as distinct peaks or valleys in the first derivative curve. Balsam and Deaton (1991, 1996) and Deaton and Balsam (1991) showed that the wavelength of a first derivative peak is unique to a particular mineral, and that the height of the peak is not only indicative of the concentration of that mineral, but also influenced by the spectral properties of the enclosing matrix.

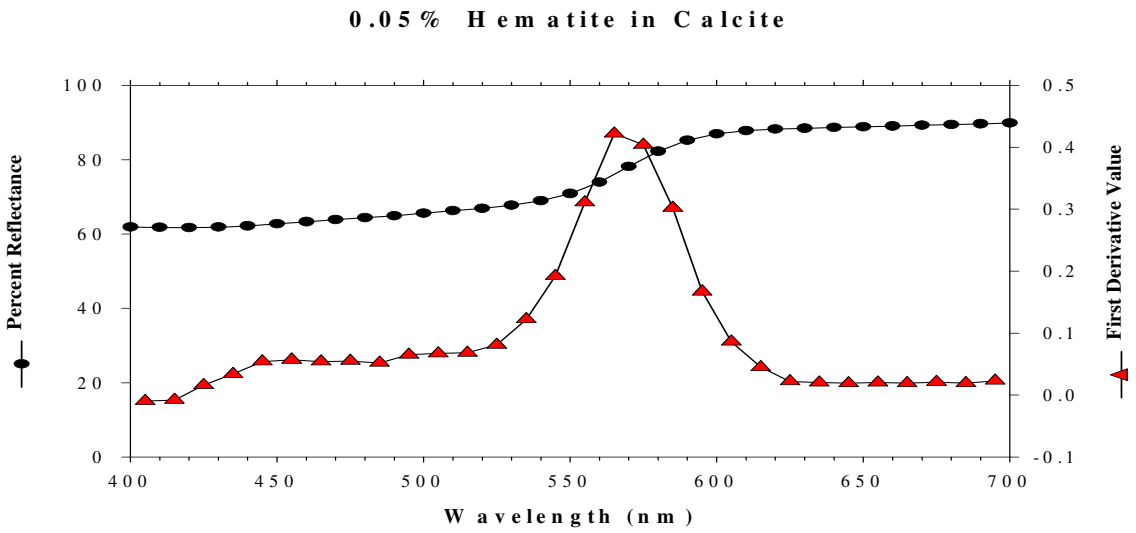

6a

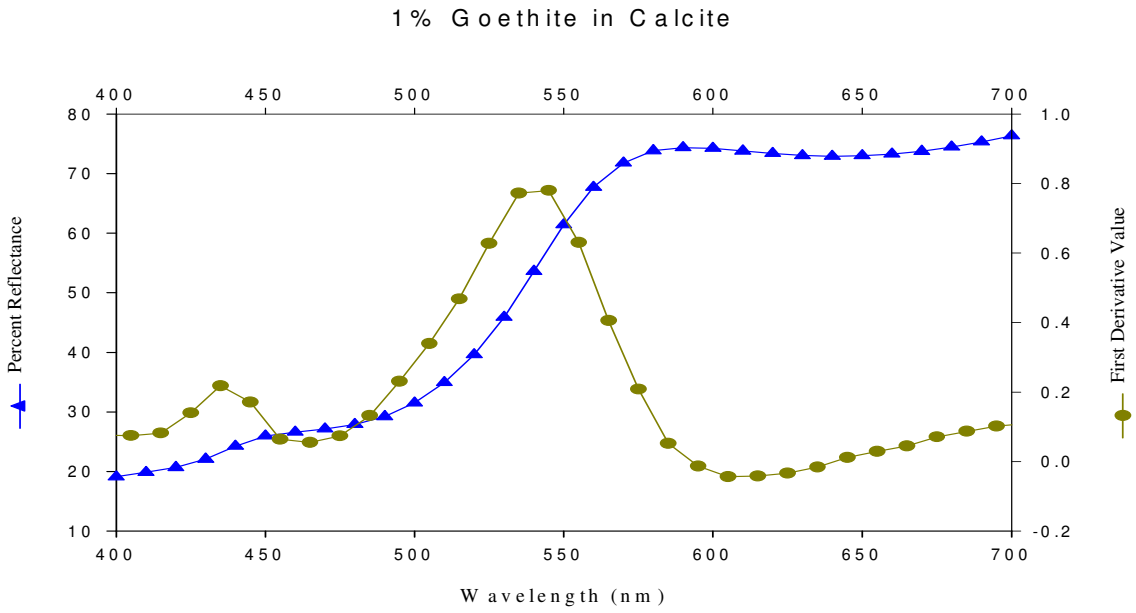

6b

Figure 6. (a) Reflectance values compared to the first derivative values for 0.05% hematite in calcite. (b) Reflectance values compared to first derivative values for 1% goethite in calcite (Balsam, personal communication).

Factor analysis was used for data reduction using SYSTAT® 10.2. Factor analysis takes an M number of variables and reduces them to N number of factors,

where ideally N is substantially less than M. It can be thought of as taking the original variables and reducing them to a few weighted averages or factors (Balsam and Deaton, 1991). In order to maximize the variance, a Varimax rotation was used during factor analysis which yielded 32 variables, one for each of the first derivative values at 10nm intervals from 395 – 705 nm for each of the 793 samples (Appendix A).

Factor analysis is an appropriate tool for analyzing reflectance spectra because it makes few assumptions about the variables used, apart from the normality of their distribution, and its results can be tested and interpreted in a number of ways. First, it can be tested by comparing the rotated factor loadings (numerical importance of each variable in a factor) to first derivative curves of known minerals or mineral combinations (Balsam and Deaton, 1991). Second, factor interpretations may be tested by comparing the rotated factor loadings with the first derivative curves of samples that have high factor scores for that factor. Samples with high scores for a factor should be end member samples, i.e., their composition should characterize that factor (Balsam and Deaton, 1991). Physical analysis (XRD, wet chemistry, etc.) of samples with a high factor scores for a factor could help interpret a factor. Third, factor scores (factor scores indicate how important a factor is in a sample) from geographically arrayed samples can be mapped and compared known distributions of sediment components. Factor scores may also provide a useful indicator of a factor's relative importance down core.

CHAPTER 5

RESULTS

5.1 Description of Factors

Factor analysis was applied to the first derivative values of VIS spectra obtained from the Simmons Core. Although initially four factors explaining 93% of the variance in the Simmons core were extracted, only Factors 2 and 3 will be used because they indicate iron oxides, namely hematite and goethite, which are useful for loess and paleosol interpretation (Balsam et al., 2005). The result of the factor analysis is presented in Table 3. The data set contains two factors that explain over 50% of the variance. However, because variance alone should not be used to determine the number of factors (Balsam and Deaton, 1991), the communality, which is the proportion of shared variance within an item and indicates the proportion of variance explained by the extracted factors of the individual variables (first derivative values at the wavelengths analyzed), as well as the variance, was used to determine the validity of the factors. The larger the communality for each variable, the more successful a factor analysis solution is (Kim and Mueller, 1978). A four factor solution was used for a number of reasons. First, the four factor solution provided a data set that resembled known minerals that are common in loess and paleosols. Second, as additional factors beyond four were extracted they provided less useful information that became increasingly

difficult to interpret. Third, plots of the factors down core appear to fit with the stratigraphy.

Rotated factor loadings (Table 3) describe how the variables, which are the first derivative wavelengths, contribute to each factor. The higher the value of the loading for a variable the more important its contribution is to a factor. Factor loadings may be positive or negative and the polarity of the factors from this data was determined by looking at each variable individually and plotting them down core.

Factor 2 (Figure 7) has one major peak centered at 565 nm with a loading of nearly 1.0. There are three other minor peaks as well. One at 685 nm with a loading of approximately 0.35, another at 495 nm with a loading of 0.1, and the third one is at 435 with a loading slightly less than 0.0.

Factor 3 (Figure 7) is positive factor and bimodal with two dominant peaks. One is between 485 and 515 nm with a loading of approximately 0.9. The other peak is centered on 435 nm and has a loading of approximately 0.78.

5.2 Description of Factor Scores Down Core

Factor scores, which indicate the importance of a factor within a sample, were calculated for each of the four factors. These scores were then plotted against the depth of the Simmons Core.

Factor 2 is a positive factor ranging from -1.7 to 3.2. Positive values for this factor occur in the paleosols and the negative to neutral values occur in the loess (Figure 8). Factor 3 is a positive factor and ranges from -2.1 to 2.8. Positive values appear

predominantly in the loess and the negative scores are dominant in the paleosols (Figure 9).

Table 3. Rotated Factor Loadings (Varimax rotation).

Variable	Factor 2	Factor 3	Communality
395	-0.195	0.506	0.918
405	-0.134	0.526	0.921
415	-0.165	0.631	0.894
425	-0.120	0.715	0.963
435	-0.028	0.759	0.980
445	-0.036	0.744	0.973
455	-0.191	0.546	0.900
465	-0.254	0.313	0.843
475	-0.281	0.639	0.934
485	0.013	0.866	0.954
495	0.121	0.923	0.985
505	0.084	0.954	0.986
515	0.093	0.977	0.988
525	0.211	0.966	0.975
535	0.472	0.869	0.985
545	0.728	0.663	0.983
555	0.892	0.420	0.981
565	0.967	0.184	0.982
575	0.979	0.053	0.988
585	0.955	-0.024	0.995
595	0.903	-0.060	0.993
605	0.771	-0.114	0.973
615	0.512	-0.188	0.930
625	0.234	-0.258	0.936
635	0.115	-0.181	0.925
645	-0.001	-0.247	0.926
655	0.019	-0.227	0.923
665	0.120	-0.211	0.902
675	0.233	-0.137	0.898
685	0.344	-0.096	0.879
695	0.300	-0.103	0.833
705	0.192	-0.147	0.803

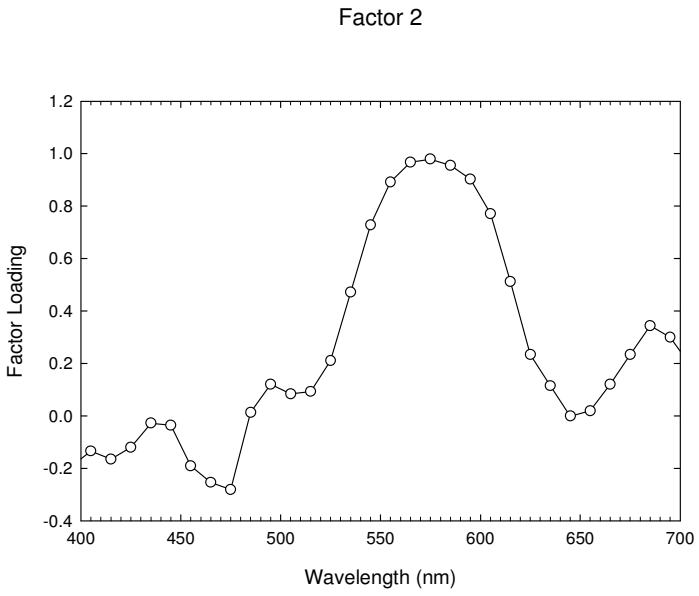

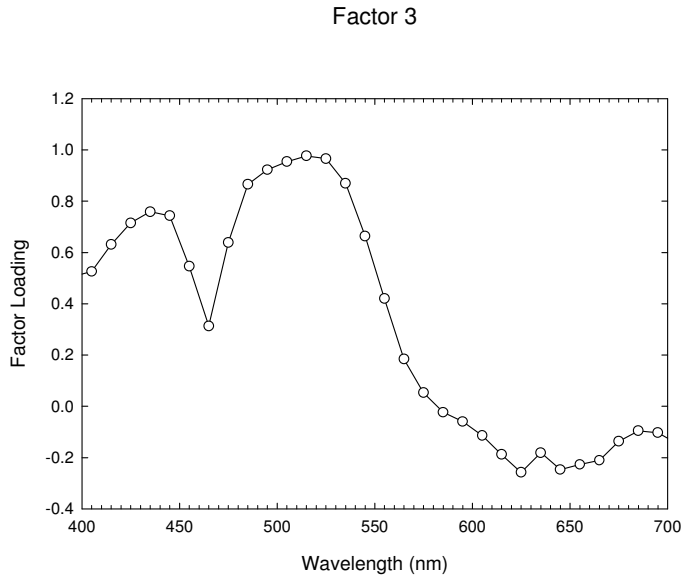

Figure 7. Graphical representation of factor loadings as a function of wavelength for two of the factors extracted from the Simmons Core.

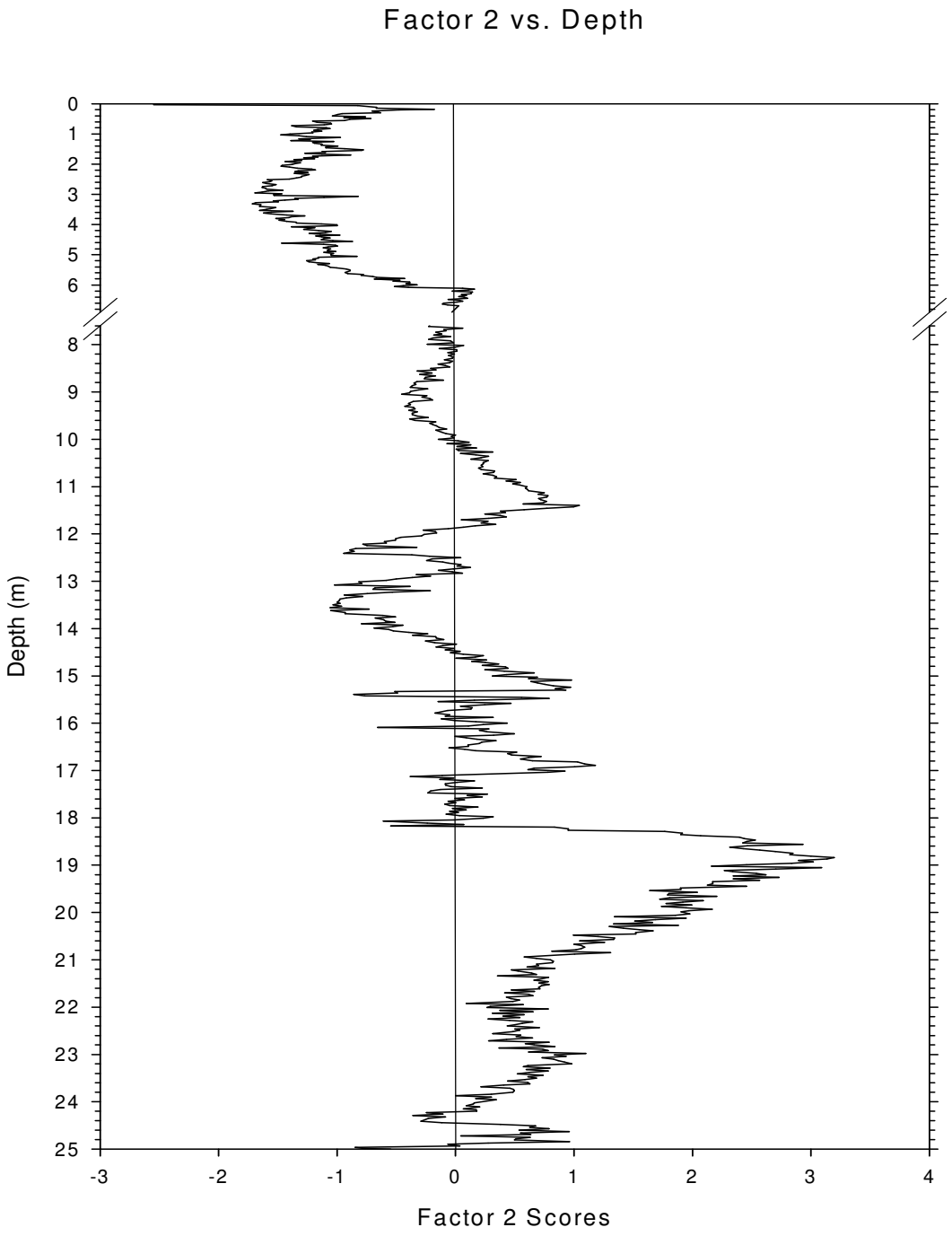

Figure 8. Factor 2 scores versus depth. The break in the data results from the missing section of the core presumed to be the Farmdale paleosol.

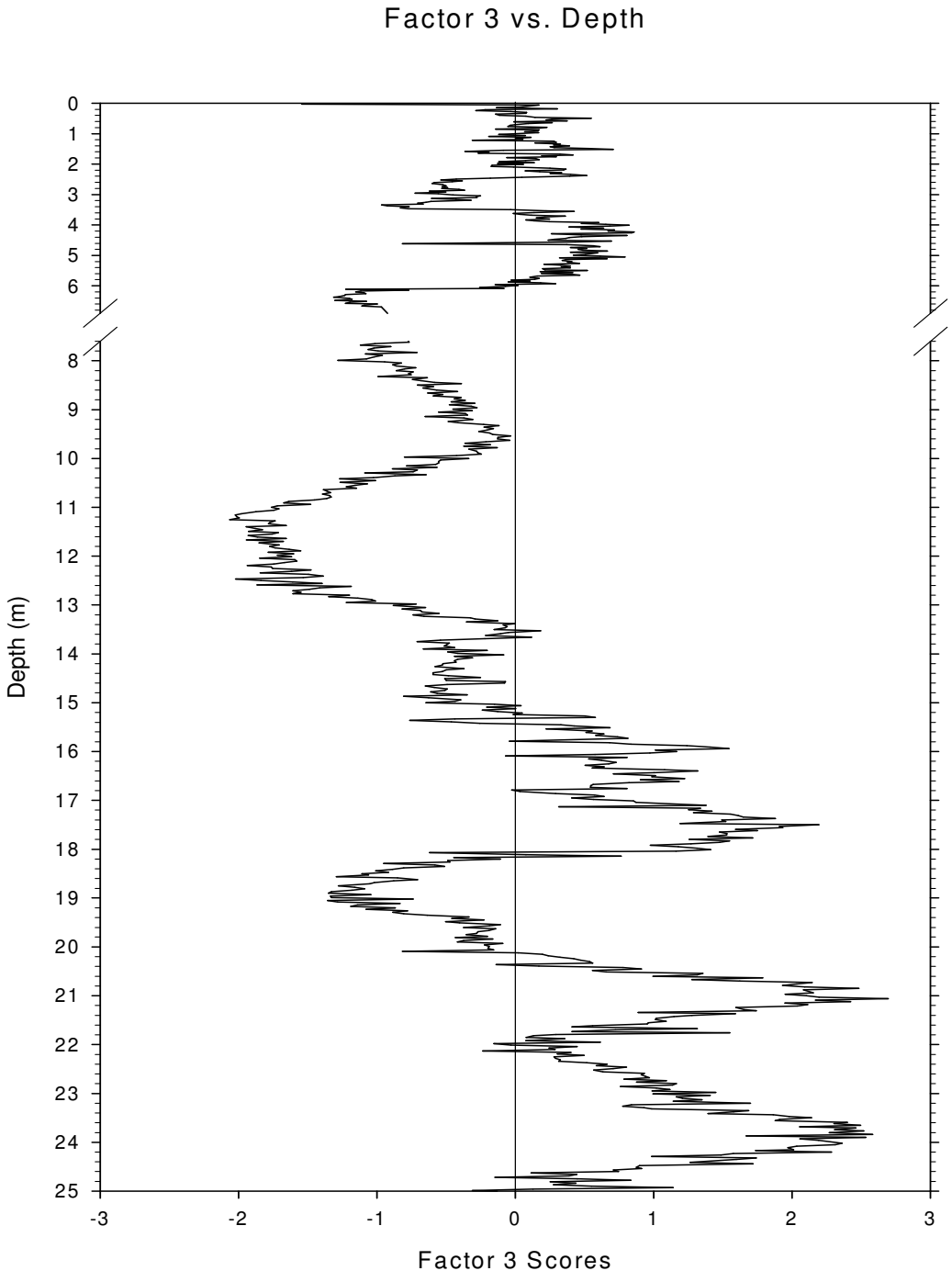

Figure 9. Factor 3 scores versus depth. The break in the data results from the missing section of the core presumed to be the Farmdale paleosol.

CHAPTER 6

DISCUSSION

6.1 Interpretation of Factors

Factor loadings relate the importance of a wavelength to a specific factor and, when plotted for the wavelength range analyzed, produce factor loading curves. Factor loading curves can be interpreted by comparison to first derivative curves of known materials. For this study, reflectance data where taken from the Simmons Core and plotted as first derivative curves which were then factor analyzed to elucidate overall assemblages of dominant wavelengths. Factors 2 and 3 were compared to known first derivative reflectance data and are interpreted as explained below.

Factor 2 is compared to 1% hematite in calcite and shows that hematite is a good match for Factor 2 (Figure 10). The secondary peak centered on 495 nm indicates a small amount of goethite mixed in with the hematite which is not surprising because hematite and goethite generally coexist in loess and paleosol sequences (Balsam, 2005). The amount of redness, or the relative importance of the red wavelengths, was also plotted for each sample down core. Data from Ji et al. (2002) uses known amounts of hematite and goethite mixed with loess and paleosol matrices to obtain calibration samples for percent reflectance of varying wavelengths. Figure 11a contains data showing a linear relationship between hematite and redness. Because hematite reflects

visible light in the red spectrum a plot of Factor 2 and redness was also used to further confirm Factor 2 as hematite (Figure 12) (Ji et al., 2002).

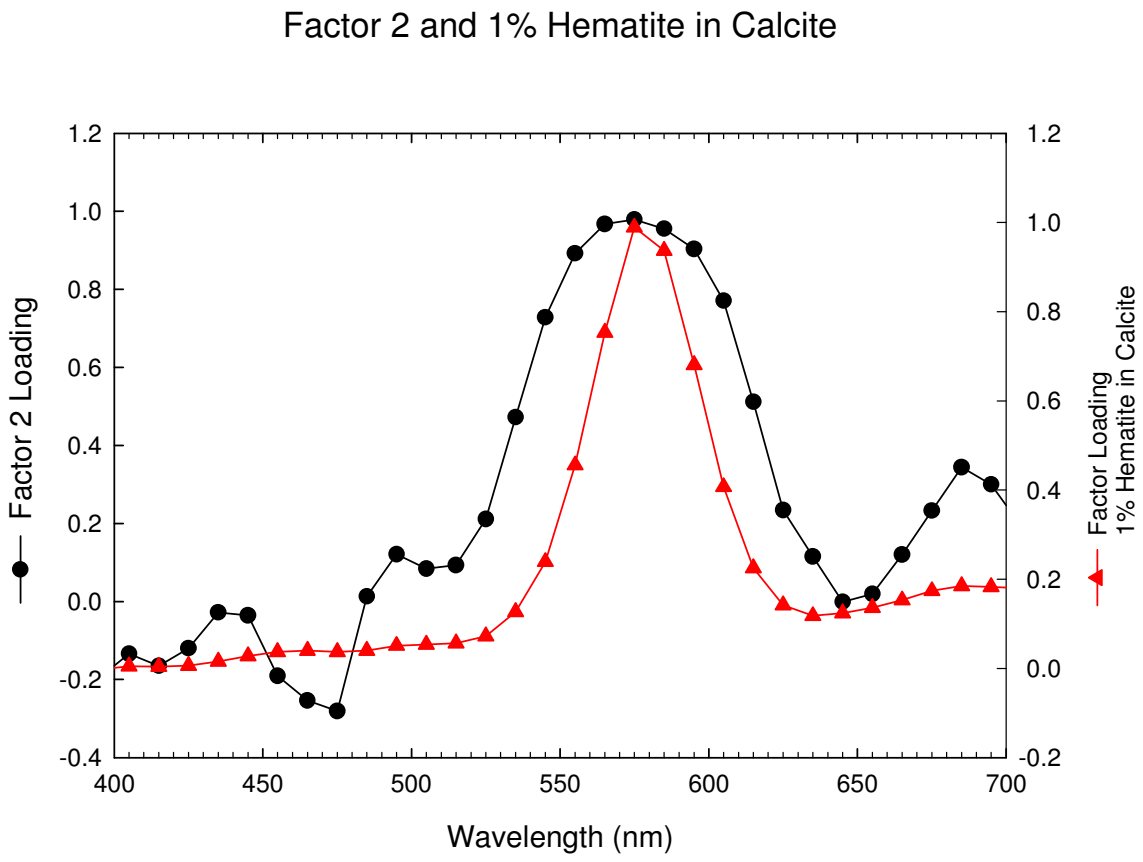

Figure 10. Comparison of factor 2 from the Simmons core data with 1% hematite in calcite (hematite data from Balsam, personal communication).

Factor 3 is interpreted as goethite and is compared to 1% goethite in calcite shown in Figure 13. Although there are slight shifts in the main peaks of Factor 3 compared to that of the standard it is not surprising because peak height, width, and position may alter slightly with varying matrix composition and/or mineral content and with the concentration of goethite (Balsam and Deaton, 1991). Figure 11b contains data

from Ji et al. (2002), showing a linear relationship between percent weight goethite and percent reflectance yellow (Ji et al., 2002). Goethite is typically a pale yellowish color and Factor 3 was compared to the percent yellow reflectance data from the Simmons core to further confirm Factor 3 as goethite (Figure 14) (Ji et al., 2002).

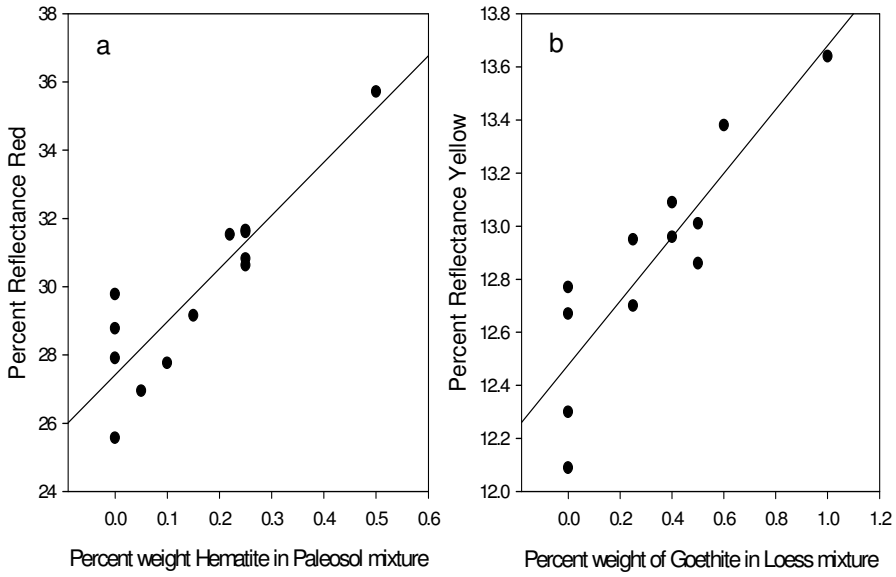

Figure 11. a. Graphical representation of percent weight hematite vs. percent reflectance of the red spectrum. b. Graphical representation of percent weight goethite vs. percent reflectance of the yellow spectrum.

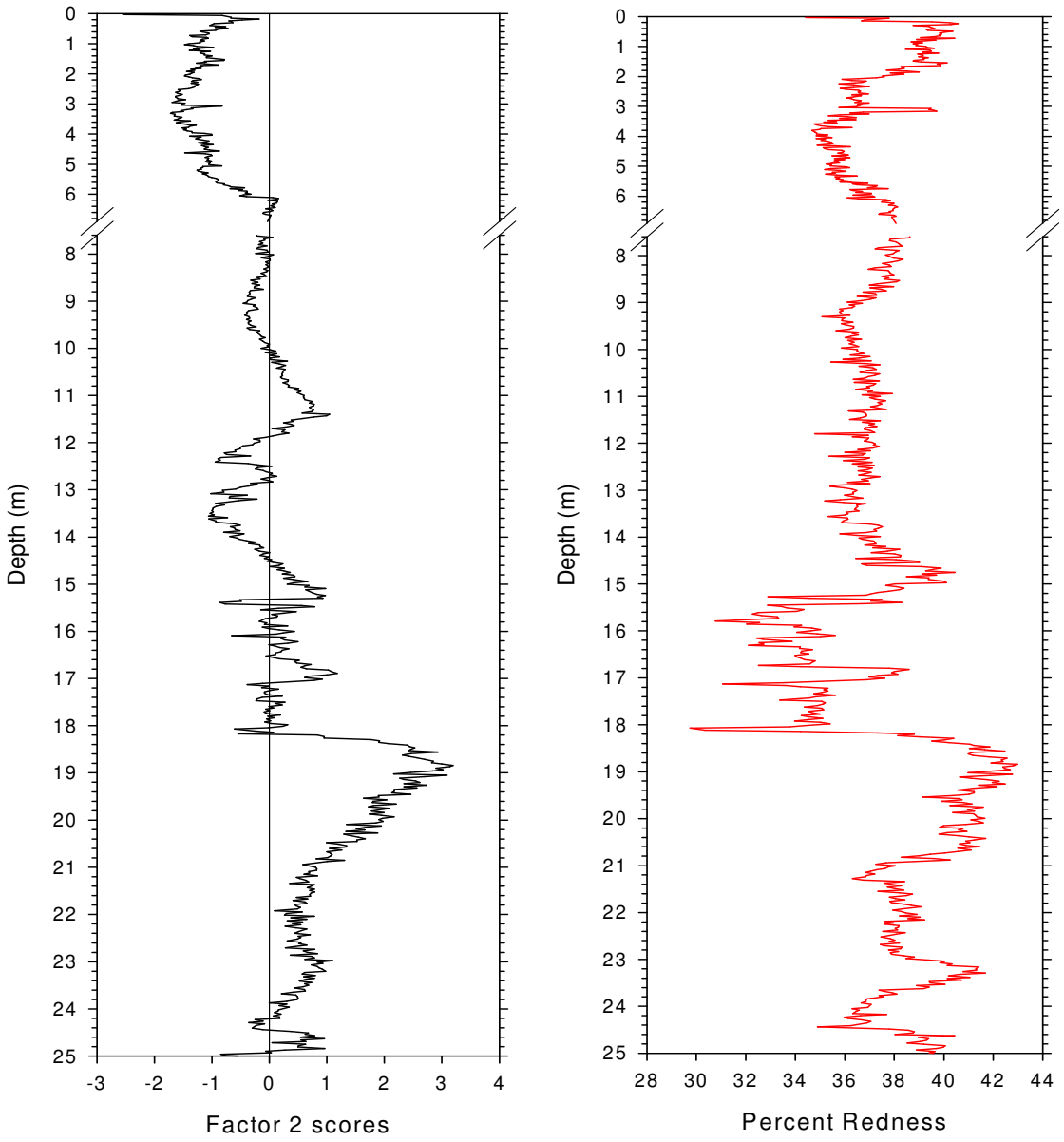

Figure 12. Factor 2 scores, which show how important (positive is more) that factor is to an individual sample are compared to the percent redness of the samples. Assuming that Factor 2 is hematite would be the best fit for the samples due to the fact that hematite reflects in the red and the relative redness intensity shows good correlation with the relative amount of hematite in the samples based on the factor scores (Torrent and Baron, 2003). The break in the data is from the missing section of the core, presumably the Farmdale interstadial paleosol.

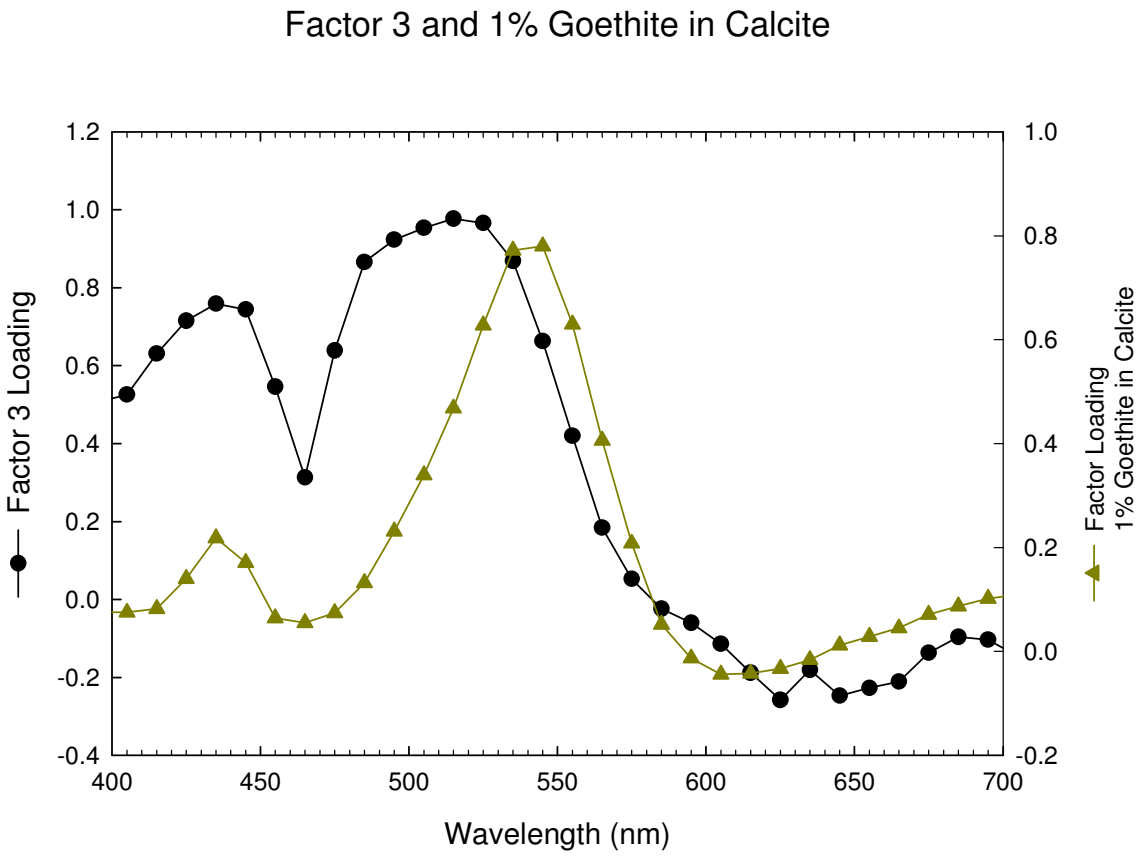

Figure 13. Comparison of Factor 3 from the Simmons core data with 1% goethite in calcite (goethite data from Balsam, personal communication).

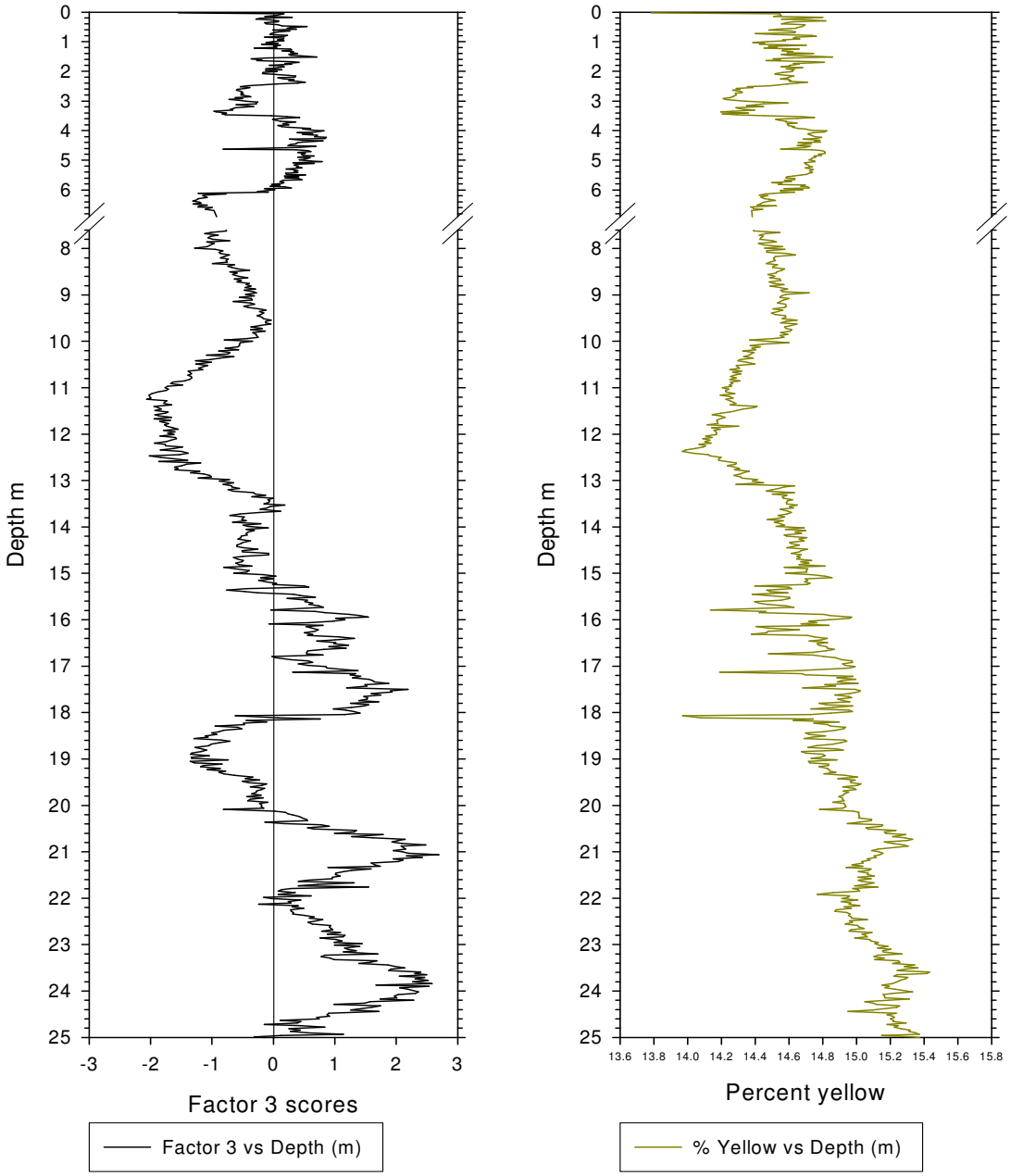

Figure 14. Factor 3 scores, which show how important (positive is more) that factor is to an individual sample are compared to the percent reflectance yellow of the samples. Assuming that Factor 3 is goethite would be the best fit for the samples due to the fact that goethite reflects in the yellow and the relative yellow intensity shows good correlation with the relative amount of goethite in the samples based on the factor scores. The break in the data is from the missing section of the core, presumably the Farmdale interstadial paleosol.

6.2 Interpretation of Factor Scores Down Core

Factor scores for Factors 2 and 3 were plotted against the lithostratigraphy of the Simmons core (Figure 15). The proposed paleosol units generally correspond to higher factor scores for hematite (Factor 2) and the loess units correspond to higher factor scores for goethite (Factor 3).

Factor 2 shows a good correlation with Paleosol 4 which is expected because hematite is generated during pedogenesis where there are alternating wet/dry conditions and good soil drainage (Schwertmann, 1971). Paleosol 4, which developed on the limestone bedrock, is probably analogous to the modern day Kansas prairie where soil thickness can be a few meters to a few centimeters above the bedrock. Paleosol 4 is considered to be a similar interglacial climate to that of today, but the soil fabric is similar to that of the Yarmouth suggesting a slightly warmer climate than today (Wang, personal communication).

The onset of the Marianna Loess (23.7-24.7m) named after its type section in the Lower Mississippi Valley and stratigraphic position in the core (Wang, personal communication), correlates with a sharp decrease in hematite and a large increase in goethite (Figure 14). The goethite data suggests a well developed glacial environment but there is some hematite production near the top of the unit from the transition glacial to interglacial.

Paleosol 3, which is presumed to be and interglacial environment, shows a good relationship with the hematite data. What is interesting to note is that there is a good amount of goethite production (~23m depth) suggesting stadial conditions within this interglacial.

This study documents the first time the Crowley's Ridge loess interval has been observed in this area. The stratigraphic interval by Hong and the goethite data match very well. There is a notable increase in the hematite and decrease in the goethite at the interval where Hong suggests an interstadial paleosol, the Prairie Du Rocher, exists confirming its presence. The hematite data shows an increase throughout the Crowley's Ridge section which could be from a gradual yet steady increase in temperature at the site where there was a transition from a full glacial interval to an interglacial one.

The Yarmouth interval contains an enormous amount of hematite suggesting a very warm to tropical environment (Schwertmann, 1971; Langmuir, 1997; Wang, personal communication). This is well established in the literature as the Yarmouth interglacial interval but it has been questioned as to whether it formed solely during on interglacial or over a longer period of time (Grimley et al., 2003). The Yarmouth has been subdivided into at least 3 different stages, two warm intervals (~20m and ~18.5m depth) and a cooler one (~19.5m depth) and these subdivisions show up in both the hematite and goethite data (Figure 15) (Lowe and Walker, 1997). Although this is a full interglacial, there was at least one period of cooling that occurred.

In the Loveland loess there is a large (1.8-1.9) factor score for goethite in this area of the core and duration (thickness) matches with Hong's visual stratigraphy.

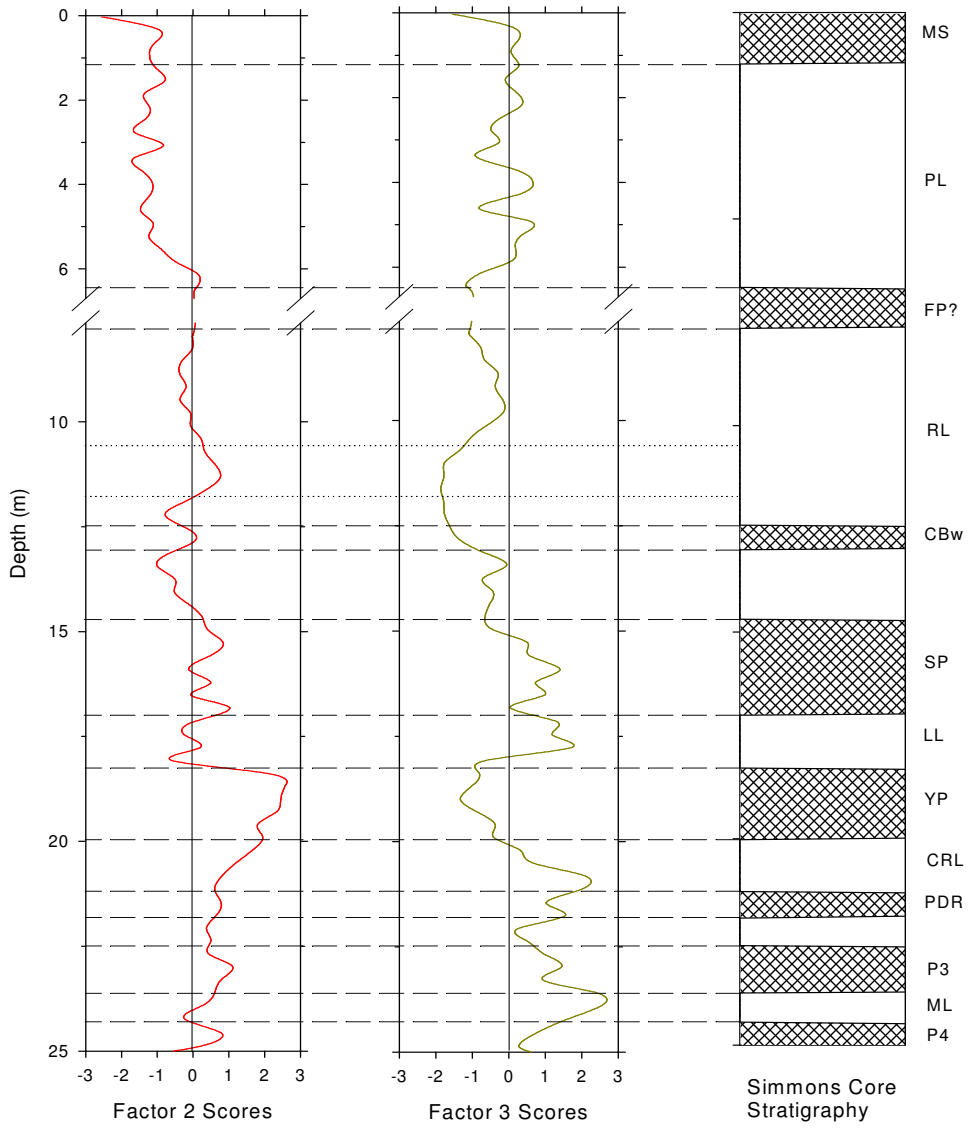

Figure 15. Factor scores for Factors 2 and 3 plotted down core compared to the Simmons core stratigraphy with the cross-hatched areas representing paleosols. The dashed lines indicate major loess/paleosol boundaries and the dotted lines indicate a proposed interstadial in the Roxana loess unit. The abbreviations to the right are as follows: MS=modern soil, PL=Peoria loess, RL=Roxana loess, CBw=Chapin paleosol, SP=Sangamon paleosol, LL=Loveland loess, YP=Yarmouth paleosol, CRL=Crowley's Ridge loess, PDR=Prairie Du Rocher paleosol, P3=Paleosol 3, ML=Marianna loess, and P4=Paleosol 4.

The Loveland loess can be correlated stratigraphically in many areas around the Midwest and is restricted to the Illinoisan glaciation (Follmer, 1996, Rutter et al., 2006). There appears to be a small spike of hematite in this interval suggesting an interstadial. The Illinoisan glacial interval was much drier and had greater fluctuations in seasonal temperature and precipitation perhaps favoring a small amount of hematite formation, but not enough to out pace goethite production and loess formation (Curry et al., 2000).

The Sangamonian interglacial is fairly well established in the literature and is used as the type section for the last full interglacial (Follmer, 1996; Hall and Anderson, 2000). This interval is correlated to the interglacial event known as oxygen isotope stage 5 which is subdivided into 5 smaller intervals "a" through "e" (Lowe and Walker, 1997, Reading, 1996). The sub stages of the stage 5 interglacial show up as three dominant hematite spikes (5a, 5c, and 5e) and two goethite spikes (5b and 5d).

The Roxana loess shows little response for goethite, which is quite surprising, as well as two distinct hematite spikes, one near the middle (~11m depth) and another near the lower boundary (~13m depth) (Figure 15). This low amount of goethite in the Roxana could be due to a number of reasons. First, much of the Roxana is dominated by quartz grains intermixed with several carbonaceous veins leading to a "bleeding out" effect of the darker minerals. Even though darker minerals will dominate the spectrum of a mixture, this effect can be nullified to some extent by the nature of the data reduction which groups the data into weighted averages (Balsam, personal communication). An interrelated and alternate explanation is a possible

change of source material to the site resulting in little or no material available for hematite and goethite production in significant quantities.

The spike near the lower boundary is most likely the interstadial paleosol Hong identifies as the Chapin Bw (Wang, personal communication). The larger (>0 factor score) and longer (~2m) interval in the middle of this section, centered near 11m depth, indicates a sustained warming event that promoted hematite formation yet prohibited paleosol development. Hematite formation in this interval could potentially be from high winds, low vegetation, and a large sediment supply coupled with periods of relative warmth or from diagenesis (Lowe and Walker, 1997).

The Peoria loess section shows multiple pulses of goethite possibly from the severe cold and dry climate during the late Wisconsian glaciation that limited goethite production (Rousseau and Kukla, 1994; Muhs and Bettis, 2000). The weathering bands noted by Hong's initial core description show up as small bumps in the hematite data confirming their existence as paleosol A horizons suggesting multiple episodes of brief soil formation.

Something that is common to all intervals is that there doesn't seem to be an overwhelmingly dominant climate signal from the mineralogy (i.e., hematite=interglacial and goethite=glacial) with the exception that hematite production was clearly dominant in the Yarmouth interval. Instead, each interval shows some change in dominant climate regimes which would imply the occurrence of multiple stadial/interstadial events. Unfortunately this section of loess and paleosol is the only North American one that has been studied in this way to date, so there is nothing else

with which to compare it to in order to confirm multiple episodes of climate change during any interval on a regional scale.

CHAPTER 7

CONCLUSIONS

1. Factor analysis produced four factors. Two of those factors were identified as being the iron oxide minerals hematite and goethite.
2. By comparing factor scores of Factors 2 and 3 with the lithostratigraphy of the Simmons core it becomes evident that there are at least four major episodes of glaciation that have been recorded at this location; Peoria/Roxana Wisconsian, Loveland Illinoisan, Crowley's Ridge Pre-Illinoisan A, and the Marianna Pre-Illinoisan B.
3. By using spectral analysis to analyze loess and paleosol a more sensitive picture of climate change can be inferred, such as in the case of the Roxana (possibly in the Loveland loess as well) loess where it shows a large interstadial development of hematite that was not noticed by other traditional methods such as visible identification, soil morphology, and Munsell colors.
4. The paleoclimatic conditions at this site inferred from the relative iron oxide content implies that over time glacial and interglacial conditions rarely reach a steady state of cold (glacial) or warm (interglacial), but instead may have brief oscillations in climate regimes that go unnoticed by other methods.

5. Further examination of other loess sequences in North America using this method could yield a more precisely correlated climate/stratigraphic interpretation and perhaps bring some consensus to North American loess stratigraphy and its relation to paleo, current, and future climate.

APPENDIX A

FACTOR SCORE DATA

Depth(m)	Factor 2	Factor 3	Depth(m)	Factor 2	Factor 3
0.0300	-2.5471	-1.5435	1.3700	-1.1324	0.2796
0.0600	-0.8254	0.1704	1.4000	-0.9960	0.3920
0.1200	-0.6672	0.0333	1.4300	-1.0940	0.2527
0.1500	-0.6663	-0.1345	1.4600	-1.0952	0.2826
0.1800	-0.1811	0.3041	1.4900	-0.9363	0.5335
0.2100	-0.4746	-0.2151	1.5200	-0.7804	0.7075
0.2400	-0.7052	-0.2834	1.5500	-0.7932	-0.0874
0.2700	-0.6577	-0.0324	1.5800	-1.1267	-0.3612
0.3000	-0.6336	0.0827	1.6100	-1.0986	-0.1900
0.3300	-0.9588	0.0770	1.6400	-1.2715	-0.2666
0.3600	-0.9939	-0.1411	1.6700	-1.1294	0.3226
0.4000	-1.0380	-0.1145	1.7000	-0.8863	0.4162
0.4300	-0.7626	0.0766	1.7300	-1.2045	0.1913
0.4600	-0.9432	0.1429	1.7600	-1.1608	0.2951
0.4900	-0.7169	0.5485	1.7900	-1.2822	-0.0618
0.5200	-0.8933	0.2655	1.8200	-1.1901	0.1471
0.5500	-0.9374	0.2226	1.8500	-1.3634	0.1738
0.5800	-1.2052	0.3741	1.8800	-1.3012	0.0755
0.6100	-1.1701	-9.7488e-3	1.9200	-1.4384	-0.1199
0.6400	-1.0563	0.2660	1.9500	-1.3102	0.1377
0.6700	-1.0476	0.0935	1.9800	-1.3535	-0.1262
0.7000	-1.1093	-1.1866e-4	2.0100	-1.3806	0.0577
0.7300	-1.3820	-0.0362	2.0400	-1.4620	-0.1669
0.7600	-1.3425	-0.0521	2.0700	-1.4730	-0.1748
0.7900	-1.0931	0.2275	2.1000	-1.4016	-0.0111
0.8200	-1.0605	0.1704	2.1300	-1.3376	0.2512
0.8500	-1.1626	-0.1415	2.1600	-1.2150	0.3659
0.8800	-1.1956	0.1712	2.1900	-1.1835	0.3485
0.9100	-1.1306	0.1610	2.2200	-1.3264	0.0721
0.9400	-1.2125	0.0673	2.2500	-1.3564	0.1775
0.9700	-1.2058	0.1686	2.2800	-1.2468	0.3330
1.0000	-1.3982	-0.0120	2.3100	-1.3610	0.2531
1.0300	-1.4753	-0.1181	2.3400	-1.2367	0.4001
1.0600	-1.3226	0.0724	2.3700	-1.2648	0.5168
1.0900	-1.2590	-0.1911	2.4000	-1.2988	0.3926
1.1200	-0.9738	0.1119	2.4300	-1.3019	0.0460
1.1600	-1.3215	4.8497e-3	2.4600	-1.3429	-0.1808
1.1900	-1.2272	0.0543	2.4900	-1.4050	-0.4259
1.2200	-1.3899	-0.3096	2.5200	-1.5882	-0.5367
1.2500	-1.0279	0.2775	2.5500	-1.5537	-0.3849
1.2800	-1.2044	0.2944	2.5800	-1.5691	-0.4556
1.3100	-1.1924	0.1424	2.6100	-1.6267	-0.5868
1.3400	-1.1295	0.3248	2.6400	-1.5979	-0.6007

Depth(m)	Factor 2	Factor 3	Depth(m)	Factor 2	Factor 3
2.6800	-1.5167	-0.5242	3.9800	-1.1326	0.6534
2.7100	-1.5499	-0.5012	4.0100	-1.0014	0.8216
2.7400	-1.6269	-0.5277	4.0400	-1.0002	0.6831
2.7700	-1.6310	-0.4889	4.0700	-1.3846	0.3890
2.8000	-1.6040	-0.5307	4.1000	-1.1877	0.6383
2.8300	-1.5918	-0.4074	4.1300	-1.2419	0.4771
2.8600	-1.4585	-0.3683	4.1600	-1.2797	0.7169
2.8900	-1.5783	-0.6200	4.2000	-1.1550	0.6717
2.9200	-1.6327	-0.5022	4.2300	-1.0510	0.8587
2.9500	-1.6924	-0.7241	4.2600	-1.0996	0.8405
2.9800	-1.4673	-0.5556	4.2900	-1.2358	0.2612
3.0100	-1.5353	-0.4501	4.3200	-1.1424	0.4763
3.0400	-1.5305	-0.2514	4.3500	-0.9788	0.8075
3.0700	-0.8231	-0.2816	4.3800	-1.1795	0.4800
3.1000	-1.1109	-0.2762	4.4100	-1.1301	0.3917
3.1300	-1.3572	-0.6055	4.4400	-1.0600	0.3654
3.1600	-1.3296	-0.4296	4.4700	-1.1121	0.2842
3.1900	-1.4412	-0.3215	4.5000	-1.1328	0.2381
3.2200	-1.5383	-0.6095	4.5300	-1.0365	0.6947
3.2500	-1.4968	-0.6445	4.5600	-0.8707	0.4328
3.2800	-1.6840	-0.7041	4.6200	-1.4665	-0.8157
3.3100	-1.7155	-0.6663	4.6500	-1.1129	0.3715
3.3400	-1.6442	-0.9653	4.6800	-1.0136	0.5658
3.3700	-1.6494	-0.9259	4.7100	-0.9977	0.6120
3.4000	-1.6542	-0.7668	4.7400	-1.0739	0.3994
3.4400	-1.5197	-0.8291	4.7700	-1.1148	0.5168
3.4700	-1.5646	-0.7737	4.8000	-1.0540	0.4542
3.5000	-1.5936	-0.0348	4.8300	-1.0702	0.4886
3.5300	-1.6540	0.2236	4.8600	-1.0829	0.6658
3.5600	-1.3728	0.4255	4.8900	-1.0113	0.3998
3.5900	-1.5544	0.1367	4.9200	-1.1126	0.5952
3.6200	-1.6195	-0.0156	4.9600	-1.0313	0.5069
3.6500	-1.5561	0.0339	4.9900	-1.0534	0.4224
3.6800	-1.4226	0.1173	5.0200	-1.0475	0.6144
3.7100	-1.2731	0.3623	5.0500	-0.8318	0.7919
3.7400	-1.3878	0.2118	5.0800	-1.1596	0.3207
3.7700	-1.4055	0.1540	5.1100	-1.1582	0.6627
3.8000	-1.5166	0.2472	5.1400	-1.2030	0.3671
3.8300	-1.4433	0.0761	5.1700	-1.1848	0.3405
3.8600	-1.4882	0.1365	5.2000	-1.2576	0.4089
3.8900	-1.4277	0.2461	5.2300	-1.2378	0.3779
3.9200	-1.3478	0.6040	5.2600	-1.1721	0.4644
3.9500	-1.3413	0.4784	5.2900	-1.0660	0.2089

Depth(m)	Factor 2	Factor 3	Depth(m)	Factor 2	Factor 3
5.3200	-1.1628	0.3300	6.6300	-0.1111	-1.0896
5.3500	-1.0979	0.3967	6.6600	-0.0663	-1.1085
5.3800	-1.0741	0.3338	6.6900	0.0246	-0.9678
5.4100	-1.0574	0.3969	7.6200	-0.2252	-0.7675
5.4400	-1.0041	0.1986	7.6500	0.0595	-1.0148
5.4700	-0.9229	0.2151	7.6800	-0.0988	-1.1184
5.5000	-0.8916	0.5219	7.7100	-0.0797	-0.9012
5.5300	-0.8904	0.1806	7.7400	-0.1670	-1.0207
5.5600	-0.9085	0.4143	7.7700	-0.1167	-1.0632
5.5900	-0.9335	0.1894	7.8000	-0.1837	-0.9902
5.6200	-0.9091	0.4072	7.8300	-0.0429	-0.7109
5.6500	-0.7800	0.4660	7.8600	-0.1900	-1.0831
5.6800	-0.7976	0.1589	7.8900	-0.2262	-0.9608
5.7200	-0.6987	0.1075	7.9200	-0.0420	-1.0199
5.7500	-0.6663	0.1730	7.9600	-0.0191	-1.0761
5.7800	-0.4306	0.1398	7.9900	-0.2400	-1.2809
5.8100	-0.6841	-0.0299	8.0200	0.0664	-0.9456
5.8400	-0.4703	0.1066	8.0500	-5.1557e-3	-0.8233
5.8700	-0.5275	-0.0500	8.0800	-0.1367	-0.8852
5.9000	-0.3901	0.1830	8.1100	8.4720e-3	-0.8603
5.9300	-0.3849	0.2911	8.1400	0.0110	-0.7187
5.9600	-0.4187	-0.1438	8.1700	-0.0630	-0.7998
5.9900	-0.3253	0.0188	8.2000	-9.9369e-3	-0.8587
6.0200	-0.4409	-0.0723	8.2300	-0.0598	-0.7376
6.0500	-0.5147	-0.2556	8.2600	-0.0205	-0.7711
6.0800	-0.3983	-0.0827	8.2900	-0.0281	-0.7525
6.1100	0.0594	-1.2250	8.3200	-0.0937	-0.9920
6.1400	0.1582	-0.7712	8.3500	-0.0252	-0.6350
6.1700	0.1092	-1.1156	8.3800	-0.0507	-0.7418
6.2000	-0.0282	-1.1529	8.4100	-0.1457	-0.6809
6.2300	0.1424	-1.0935	8.4400	-0.0878	-0.5825
6.2600	0.1328	-1.0794	8.4700	-0.0506	-0.3907
6.2900	0.1299	-1.2255	8.5000	-0.2108	-0.7076
6.3200	0.0496	-1.2330	8.5300	-0.1661	-0.5915
6.3500	0.0923	-1.2743	8.5600	-0.3220	-0.6658
6.3800	0.0274	-1.3115	8.6000	-0.1996	-0.5680
6.4100	0.0705	-1.1989	8.6300	-0.3026	-0.4177
6.4400	0.1007	-1.1789	8.6600	-0.1708	-0.6329
6.4800	-0.0613	-1.3034	8.6900	-0.2538	-0.5238
6.5100	0.0320	-1.0763	8.7200	-0.2619	-0.5904
6.5400	0.0590	-1.1957	8.7500	-0.1028	-0.3934
6.5700	0.0112	-1.2268	8.7800	-0.3270	-0.4415
6.6000	-0.1000	-0.9969	8.8100	-0.3507	-0.3622

Depth(m)	Factor 2	Factor 3	Depth(m)	Factor 2	Factor 3
8.8400	-0.3371	-0.4625	10.150	0.0140	-0.7857
8.8700	-0.3638	-0.2937	10.180	0.1745	-0.5668
8.9000	-0.3812	-0.4754	10.210	6.2745e-3	-0.8876
8.9300	-0.2377	-0.3185	10.240	0.0259	-0.7086
8.9600	-0.3144	-0.2774	10.270	0.3133	-0.7385
8.9900	-0.3789	-0.4508	10.300	0.0429	-1.0861
9.0200	-0.3895	-0.3116	10.330	0.1705	-0.6456
9.0500	-0.4553	-0.5523	10.360	0.2787	-0.8695
9.0800	-0.2443	-0.3599	10.390	0.2151	-1.0237
9.1100	-0.2826	-0.3450	10.420	0.1302	-1.2690
9.1400	-0.2175	-0.6527	10.450	0.2738	-1.0113
9.1700	-0.1952	-0.3716	10.490	0.2333	-1.2639
9.2000	-0.3574	-0.3067	10.520	0.2330	-1.0691
9.2400	-0.3952	-0.4827	10.550	0.2177	-1.1557
9.2700	-0.3810	-0.4136	10.580	0.2288	-1.2200
9.3000	-0.4289	-0.2286	10.610	0.1961	-1.1487
9.3300	-0.3545	-0.1186	10.640	0.2172	-1.3867
9.3600	-0.3416	-0.2252	10.670	0.3285	-1.3614
9.3900	-0.3940	-0.1578	10.700	0.3216	-1.3350
9.4200	-0.3239	-0.2031	10.730	0.2344	-1.3915
9.4500	-0.3664	-0.2628	10.760	0.3134	-1.3405
9.4800	-0.3655	-0.1851	10.7900	0.3454	-1.3299
9.5100	-0.3221	-0.1622	10.8200	0.3277	-1.3622
9.5400	-0.2320	-0.0346	10.8500	0.5090	-1.4524
9.5700	-0.3875	-0.1237	10.8800	0.4271	-1.6375
9.6000	-0.3422	-0.1275	10.9100	0.5462	-1.6722
9.6300	-0.1686	-0.0394	10.9400	0.4841	-1.4801
9.6600	-0.2175	-0.2119	10.9700	0.5409	-1.7192
9.6900	-0.1889	-0.3634	11.0000	0.6009	-1.7610
9.7200	-0.1615	-0.1800	11.0300	0.5898	-1.7077
9.7500	-0.1360	-0.3710	11.0600	0.6039	-1.7444
9.7800	-0.0762	-0.1315	11.0900	0.6154	-1.8737
9.8100	-0.1669	-0.3347	11.1300	0.7480	-1.9790
9.8500	-0.1164	-0.2801	11.1600	0.6964	-2.0235
9.8800	-0.0812	-0.2720	11.1900	0.7799	-2.0131
9.9100	-1.0321e-3	-0.2470	11.2200	0.7677	-1.9952
9.9400	-0.0352	-0.4242	11.2500	0.7014	-2.0632
9.9700	-0.0142	-0.7994	11.2800	0.7185	-1.7361
10.000	-0.1437	-0.3384	11.3100	0.7665	-1.7749
10.030	0.0204	-0.5400	11.3400	0.7401	-1.7828
10.060	0.1110	-0.5527	11.3700	0.5710	-1.6552
10.090	-0.0711	-0.5532	11.4000	1.0434	-1.9434
10.120	0.1273	-0.5751	11.4300	0.9952	-1.8788

Depth(m)	Factor 2	Factor 3	Depth(m)	Factor 2	Factor 3
11.4600	0.7694	-1.8275	12.7700	-0.1448	-1.6059
11.4900	0.5774	-1.9261	12.8000	-0.0279	-1.1985
11.5200	0.3786	-1.7129	12.8300	0.0567	-1.3476
11.5500	0.4202	-1.7578	12.8600	-0.3309	-1.1370
11.5800	0.2468	-1.9301	12.8900	-0.2133	-1.0371
11.6100	0.3769	-1.8640	12.9200	-0.3663	-1.0103
11.6400	0.4284	-1.6559	12.9500	-0.5009	-1.2212
11.6700	0.2802	-1.9421	12.9800	-0.5861	-0.7167
11.7000	0.0489	-1.6765	13.0100	-0.8159	-0.8811
11.7300	0.2722	-1.8501	13.0500	-0.7919	-0.6488
11.7700	0.2163	-1.7062	13.0800	-1.0220	-0.8176
11.8000	0.3378	-1.7737	13.1100	-0.3836	-0.6847
11.8300	0.1668	-1.7352	13.1400	-0.6798	-0.6741
11.8600	0.0647	-1.6353	13.1700	-0.6975	-0.5511
11.8900	-0.0601	-1.5525	13.2000	-0.2144	-0.7381
11.9200	-0.2736	-1.7853	13.2300	-0.5342	-0.6600
11.9500	-0.1700	-1.6014	13.2600	-0.7455	-0.3246
11.9800	-0.1614	-1.7201	13.2900	-0.9386	-0.2901
12.0100	-0.2652	-1.6169	13.3200	-0.7850	-0.1274
12.0400	-0.2872	-1.8474	13.3500	-0.9228	-0.3515
12.0700	-0.4621	-1.5940	13.3800	-0.9768	-2.5383e-3
12.1000	-0.5053	-1.5786	13.4100	-0.9827	-0.0868
12.1300	-0.5089	-1.6686	13.4400	-0.9991	-0.0583
12.1600	-0.5994	-1.7438	13.4700	-0.9768	-0.0739
12.1900	-0.5845	-1.9368	13.5000	-1.0341	-0.1528
12.2200	-0.7824	-1.7639	13.5300	-0.9632	0.1834
12.2500	-0.7474	-1.7529	13.5600	-1.0590	-0.0493
12.2800	-0.3299	-1.4779	13.5900	-0.7309	-0.1063
12.3100	-0.8415	-1.6178	13.6200	-1.0527	-0.2142
12.3400	-0.8918	-1.8410	13.6600	-0.9310	0.1186
12.3700	-0.8578	-1.4948	13.6900	-0.9331	-0.2204
12.4100	-0.9440	-1.3882	13.7200	-0.6139	-0.5420
12.4400	-0.3680	-1.5317	13.7500	-0.5071	-0.7086
12.4700	-0.2209	-2.0212	13.7800	-0.6779	-0.4769
12.5000	0.0420	-1.8387	13.8100	-0.6066	-0.4955
12.5300	-0.1973	-1.6083	13.8400	-0.5918	-0.5132
12.5600	-0.2425	-1.3975	13.8700	-0.5125	-0.4399
12.5900	-0.1063	-1.8667	13.9000	-0.7931	-0.6645
12.6200	-0.0593	-1.1858	13.9300	-0.4460	-0.2034
12.6500	0.0458	-1.4137	13.9600	-0.5297	-0.4880
12.6800	0.0119	-1.4875	13.9900	-0.6864	-0.4147
12.7100	0.1259	-1.6064	14.0200	-0.5643	-0.0846
12.7400	-0.0192	-1.5487	14.0500	-0.5247	-0.4402

Depth(m)	Factor 2	Factor 3	Depth(m)	Factor 2	Factor 3
14.0800	-0.3941	-0.3093	15.3900	-0.8597	-0.4608
14.1100	-0.2350	-0.4143	15.4200	-0.7659	-0.2557
14.1400	-0.3622	-0.4398	15.4500	0.5549	0.3296
14.1700	-0.1687	-0.4295	15.4800	0.7871	0.4256
14.2000	-0.1596	-0.5218	15.5100	0.1585	0.6851
14.2300	-0.0995	-0.5279	15.5400	-0.1468	0.2230
14.2600	-0.2527	-0.5796	15.5800	0.4656	0.5546
14.3000	-0.1759	-0.3716	15.6100	0.2464	0.5122
14.3300	5.7422e-3	-0.4970	15.6400	0.0418	0.6386
14.3600	-0.1063	-0.5276	15.6700	0.1388	0.5820
14.3900	-0.1648	-0.5944	15.7000	0.1304	0.7380
14.4200	-0.0164	-0.5937	15.7300	-0.0665	0.8135
14.4500	-0.0853	-0.4839	15.7900	-0.1727	-0.0422
14.4800	0.0378	-0.2532	15.8200	-0.0492	0.6825
14.5100	-0.0429	-0.5095	15.8500	-0.0875	0.8346
14.5400	0.0648	-0.4974	15.8800	0.3156	1.2415
14.5700	0.2339	-0.0721	15.9100	-0.1197	1.4099
14.6000	0.1644	-0.0787	15.9400	-5.7283e-3	1.5450
14.6300	4.3303e-3	-0.4925	15.9700	0.1713	1.0139
14.6600	0.2604	-0.6498	16.0000	0.4343	1.1670
14.6900	0.1361	-0.5847	16.0300	0.2347	0.9721
14.7200	0.2521	-0.4915	16.0600	0.1083	0.5751
14.7500	0.3615	-0.5082	16.0900	-0.6567	-0.0690
14.7800	0.2259	-0.6111	16.1200	0.2789	0.8070
14.8100	0.4202	-0.5648	16.1500	0.2016	0.5321
14.8400	0.4427	-0.3490	16.1800	0.2623	0.6239
14.8700	0.2471	-0.8062	16.2200	0.4962	0.7286
14.9000	0.4109	-0.6253	16.2500	0.3221	0.6750
14.9400	0.6628	-0.3955	16.2800	-4.0318e-3	0.5060
14.9700	0.4291	-0.4334	16.3100	0.0920	0.6409
15.0000	0.3118	-0.6451	16.3400	0.1800	0.5569
15.0300	0.6899	-0.1493	16.3700	0.3391	1.0799
15.0600	0.6168	0.0399	16.4000	0.2218	1.3191
15.0900	0.9775	-0.2061	16.4300	0.1991	1.0029
15.1200	0.6356	2.0305e-3	16.4600	0.1056	0.7087
15.1500	0.6912	-0.2371	16.4900	0.1070	1.0130
15.1800	0.7516	-0.1276	16.5200	-0.0545	0.9886
15.2100	0.8245	0.0503	16.5500	0.0746	1.2240
15.2400	0.9717	-0.0134	16.5800	0.1675	0.9040
15.2700	0.8410	0.5049	16.6100	0.5151	1.1840
15.3000	0.9297	0.5787	16.6400	0.4385	0.8215
15.3300	-0.5126	-0.4371	16.6700	0.4734	0.5634
15.3600	-0.4909	-0.7632	16.7000	0.7226	0.5455

Depth(m)	Factor 2	Factor 3	Depth(m)	Factor 2	Factor 3
16.7300	0.6171	0.5429	18.0700	-0.6093	-0.6197
16.7600	0.5499	0.8077	18.1100	-0.2391	0.0759
16.7900	0.6482	-0.0252	18.1400	0.0675	0.7651
16.8200	1.0292	0.0350	18.1700	-0.5465	-0.4439
16.8600	1.0881	0.2919	18.2000	0.8348	-0.1085
16.8900	1.1795	0.5712	18.2300	0.9513	-0.4875
16.9200	1.0043	0.6426	18.2600	0.9496	-0.4717
16.9500	0.6635	0.4068	18.2900	1.7653	-0.9500
16.9800	0.6114	0.5649	18.3200	1.9133	-0.5813
17.0100	0.9228	0.8551	18.3500	1.9019	-0.5121
17.0400	0.7796	0.8725	18.3800	2.0677	-0.8060
17.1000	-0.1146	1.3791	18.4100	2.3960	-0.8857
17.1300	-0.3834	0.3141	18.4400	2.4369	-1.0074
17.1600	-0.0159	1.3375	18.4700	2.5296	-0.9174
17.1900	-0.1327	1.2519	18.5000	2.4595	-1.1078
17.2200	0.1575	1.4201	18.5300	2.4238	-1.0618
17.2500	0.0131	1.2893	18.5600	2.9305	-1.2931
17.2800	-0.0868	1.5573	18.5900	2.4633	-0.8498
17.3100	-0.0838	1.6110	18.6200	2.3148	-0.7060
17.3400	-0.0389	1.6469	18.6500	2.4261	-0.8791
17.3700	0.2241	1.8791	18.6800	2.5667	-1.0177
17.4000	-0.1284	1.4925	18.7100	2.6982	-1.0494
17.4300	-0.2105	1.5212	18.7500	2.8472	-1.2780
17.4700	-0.2332	1.1926	18.7800	2.8225	-1.1593
17.5000	0.2690	2.1931	18.8100	2.9986	-1.0873
17.5300	0.0971	1.9090	18.8400	3.1947	-1.1791
17.5600	0.2234	1.9308	18.8700	3.1353	-1.3290
17.5900	-4.3702e-3	1.5934	18.9000	2.8952	-1.3501
17.6200	0.0739	1.7492	18.9300	3.0173	-1.0438
17.6500	-0.0621	1.4752	18.9600	2.8361	-1.3344
17.6800	2.8959e-3	1.5295	18.9900	2.4548	-1.3284
17.7100	-0.0901	1.5267	19.0200	2.1615	-0.7386
17.7400	-0.0493	1.3926	19.0500	3.0888	-1.3564
17.7700	0.1884	1.7150	19.0800	2.7026	-1.2845
17.8000	-0.0263	1.2566	19.1100	2.2693	-0.8340
17.8300	0.0872	1.5480	19.1400	2.3393	-1.1403
17.8600	-0.0506	1.4796	19.1700	2.5397	-1.1870
17.8900	0.0226	1.2699	19.2000	2.6181	-0.8665
17.9200	-0.0784	0.9756	19.2300	2.3451	-1.0780
17.9500	0.0311	1.1786	19.2600	2.7316	-0.7798
17.9800	0.3166	1.3134	19.2900	2.3444	-0.8856
18.0100	0.2347	1.4128	19.3200	2.5642	-0.8058
18.0400	-0.0127	1.1627	19.3500	2.1712	-0.6351

Depth(m)	Factor 2	Factor 3	Depth(m)	Factor 2	Factor 3
19.3900	2.1694	-0.3360	20.7000	1.0593	1.6226
19.4200	2.1281	-0.4585	20.7300	1.0897	2.1434
19.4500	2.4566	-0.2261	20.7600	1.0604	2.0334
19.4800	1.8977	-0.5037	20.7900	1.0153	1.9314
19.5100	1.9020	-0.4042	20.8200	0.8128	2.0927
19.5400	1.6388	-0.1088	20.8500	1.3071	2.4824
19.5700	2.0375	-0.1852	20.8800	1.0053	2.0829
19.6000	1.8010	-0.3721	20.9400	0.5808	2.1537
19.6300	1.7892	-0.1427	20.9700	0.6831	1.9511
19.6600	2.2035	-0.1899	21.0000	0.8015	2.1041
19.6900	1.8064	-0.2700	21.0300	0.8261	2.1969
19.7200	1.7243	-0.2793	21.0600	0.8179	2.6949
19.7500	2.0917	-0.3538	21.0900	0.6857	2.1708
19.7800	1.9182	-0.2007	21.1200	0.6979	2.4222
19.8100	1.7779	-0.4332	21.1500	0.6038	1.9497
19.8400	1.9933	-0.1639	21.1800	0.8386	2.1136
19.8700	1.7400	-0.3744	21.2100	0.4709	2.0389
19.9000	1.9470	-0.4182	21.2400	0.5274	1.5957
19.9300	2.1659	-0.0906	21.2800	0.6411	1.6535
19.9600	1.9697	-0.2227	21.3100	0.6830	1.7412
19.9900	1.9039	-0.1883	21.3400	0.3549	0.8888
20.0300	1.9768	-0.1965	21.3700	0.7841	1.5910
20.0600	1.8559	-0.1567	21.4000	0.7285	1.2766
20.0900	1.3405	-0.8142	21.4300	0.6618	1.1466
20.1200	1.9460	0.0216	21.4600	0.7804	1.0208
20.1500	1.6885	0.1963	21.4900	0.7036	1.0123
20.1800	1.5126	0.2382	21.5200	0.7875	1.0887
20.2100	1.6617	0.3223	21.5500	0.7268	0.9630
20.2400	1.3337	0.4231	21.5800	0.7018	0.9549
20.2700	1.8785	0.4710	21.6100	0.7119	0.5583
20.3000	1.2973	0.5371	21.6400	0.4706	0.4094
20.3300	1.4159	0.5588	21.6700	0.6644	1.3142
20.3600	1.5496	-0.1374	21.7000	0.4156	0.7253
20.3900	1.6669	0.1699	21.7300	0.6156	0.4098
20.4200	1.5199	0.7792	21.7600	0.6533	1.5514
20.4500	1.5216	0.9109	21.7900	0.4301	0.2932
20.4800	0.9930	0.5596	21.8200	0.4662	0.1327
20.5100	1.2037	0.6569	21.8500	0.5391	0.0799
20.5400	1.3421	1.3557	21.8800	0.4833	0.3569
20.5700	1.3331	1.3146	21.9200	0.0911	0.0780
20.6000	1.0474	0.9957	21.9500	0.5700	0.6144
20.6300	1.2564	1.7890	21.9800	0.2953	-0.1554
20.6700	0.9991	1.2774	22.0100	0.2645	-0.0301

Depth(m)	Factor 2	Factor 3	Depth(m)	Factor 2	Factor 3
22.0400	0.7801	0.4475	23.3500	0.7810	1.6866
22.0700	0.3731	0.2446	23.3800	0.6204	1.5790
22.1000	0.6520	0.2859	23.4100	0.5211	1.3929
22.1300	0.3120	-0.2363	23.4400	0.7377	1.8648
22.1600	0.5772	0.4012	23.4700	0.6122	1.9788
22.1900	0.3999	0.3043	23.5000	0.6808	2.1407
22.2200	0.5432	0.4973	23.5300	0.5856	1.9125
22.2500	0.2736	0.2806	23.5600	0.4410	1.8790
22.2800	0.4553	0.2912	23.5900	0.6088	2.3990
22.3100	0.6502	0.3263	23.6200	0.6256	2.3043
22.3400	0.5630	0.3136	23.6500	0.4068	2.4947
22.3700	0.5004	0.5164	23.6800	0.2142	2.0549
22.4000	0.4369	0.6629	23.7100	0.4591	2.4622
22.4300	0.7050	0.5866	23.7400	0.4876	2.3085
22.4600	0.5001	0.8039	23.7700	0.4963	2.5199
22.4900	0.5431	0.7077	23.8000	0.4829	2.2707
22.5200	0.4832	0.5683	23.8400	0.3025	2.5826
22.5600	0.3149	0.6339	23.8700	4.3484e-4	1.6702
22.5900	0.5487	0.9327	23.9000	0.3020	2.5334
22.6200	0.5124	0.9113	23.9300	0.1705	2.0577
22.6500	0.6484	0.9391	23.9600	0.3426	2.1918
22.6800	0.4291	0.9676	24.0200	0.1584	2.3614
22.7100	0.2793	0.7856	24.0500	0.1488	2.3118
22.7400	0.7894	1.0911	24.0800	0.0910	2.0352
22.7700	0.5909	0.8784	24.1100	0.2010	1.9697
22.8000	0.6631	1.1632	24.1500	0.0665	2.0112
22.8300	0.8368	1.1371	24.1700	0.1735	1.7369
22.8600	0.3681	0.7610	24.2000	0.1791	2.2839
22.8900	0.7365	1.0202	24.2300	-0.2451	1.5755
22.9200	0.7816	1.1183	24.2600	-0.1081	1.4858
22.9500	0.6160	0.9908	24.2900	-0.3609	0.9856
22.9800	1.0996	1.4481	24.3200	-0.0852	1.7421
23.0100	0.8336	0.9962	24.3500	-0.2306	1.5967
23.0400	0.9307	1.4076	24.4100	-0.2926	1.2630
23.0700	0.7323	1.1629	24.4400	-0.1177	1.7194
23.1000	0.8277	1.2082	24.4800	0.3786	0.8997
23.1300	0.8658	1.3485	24.5100	0.6743	0.8757
23.1600	0.9195	1.1415	24.5400	0.6254	0.9138
23.2000	0.9808	1.7002	24.5700	0.7897	0.7093
23.2300	0.6133	0.8392	24.6000	0.5367	0.7462
23.2600	0.5727	0.7781	24.6300	0.9567	0.1150
23.2900	0.7965	0.9297	24.6600	0.5499	0.4443
23.3200	0.5975	0.9843	24.6900	0.6336	0.3898

24.7200	0.0458	-0.1457	24.9000	-0.0636	0.5517
24.7500	0.6294	0.4477	24.9300	0.0342	1.1411
24.7800	0.5091	0.8341	24.9600	-0.8465	0.1272
24.8100	0.4975	0.2538	24.9900	-0.7673	-0.3097
24.8400	0.9614	0.4386	25.0200	-0.1093	0.2252
24.8700	0.2738	0.2762	25.0500	-0.8942	0.8076

REFERENCES

Balsam, W.L., and Wolhart, R.J., 1993, Sediment Dispersal in the Argentine Basin: evidence from visible light spectra: Deep Sea Research II, v. 40, no. 4/5, p. 1001-1031.

Balsam, W.L., Otto-Bleisner, B.L., and Deaton, B.C., 1995, Modern and last glacial maximum eolian sedimentation patterns in the Atlantic Ocean interpreted from sediment iron oxide content: Paleoceanography, v. 10, no. 3, p. 493-507.

Balsam, W.L., and Deaton, B.C., 1991, Sediment Dispersal in the Atlantic Ocean: Evaluation By Visible Light Spectra: Reviews in Aquatic Sciences, v. 4(4), p. 411-477.

Balsam, W.L., and Deaton, B.C., 1996, Determining the composition of late Quaternary marine sediments from NUV, VIS, and NIR diffuse reflectance spectra: Marine Geology, v. 134, p. 31-55.

Balsam, W.L., and Beeson, J.P., 2003, Sea-floor sediment distribution in the Gulf of Mexico: Deep Sea Research I, v. 50, p. 1421-1444.

Balsam, W.L., Ji, J., Chen, J., 2004, Climatic interpretation of the Luochan and Lingtai loess sections, China, based on changing iron oxide mineralogy and magnetic susceptibility: Earth and Planetary Science Letters, v. 223, p. 335-348.

Balsam, W.L., Ellwood, B., and Ji, J., 2005, Direct correlation of the marine oxygen isotope record with Chinese Loess Plateau iron oxide and magnetic susceptibility records: Paleogeography, Paleoclimatology, Paleoecology, v. 221, p. 141-152.

Barranco, F.T. Jr., Balsam, W.L., and Deaton, B.C., 1989, Quantitative Reassessment of Brick Red Lutites: Evidence From Reflectance Spectrophotometry: Marine Geology, v. 89, p. 299-314.

Blinnikov, M., Busacca, A., Whitlock, C., 2002, Reconstruction of late Pleistocene grassland of the Columbia Basin, Washington, USA, based on pytolith records in loess: Paleogeography, Paleoclimatology, Paleoecology, v. 177, p. 77-101.

Chen, J., Ji, J., Balsam, W.L., Chen, Y., Liu, L., and An, Z., 2002, Characterization of the Chinese loess-paleosol stratigraphy by whiteness measurement: Paleogeography, Paleoclimatology, Paleoecology, v. 183, p. 287-297.

Clark, R.N., 1995, Reflectance Spectra: Rock Physics and Phase Relations A Handbook of Physical Constants AGU Reference Shelf 3, American Geophysical Union, p. 178-188.

Costantini, E.A.C., Lessovaia, S., and Vodyanitskii, Y., 2006, Using the analysis of iron and iron oxides in paleosols (TEM, geochemistry, and iron forms) for the assessment of present and past pedogenesis: Quaternary International, v. 156-157, p. 200-211.

Curry, B.B., and Pavich, M.J., 1996, Absence of Glaciation in Illinois during Marine Isotope Stages 3 through 5: Quaternary Research, v. 46, p. 19-26.

Curry, B.B., and Baker, R.G., 2000, Palaeohydrology, vegetation, and climate since the late Illinois Episode (~130 ka) in south-central Illinois: Paleogeography, Paleoclimatology, Paleoecology, v. 155, p. 59-81.

Davis, L.G., Muehlenbachs, K., Schweger, C.E., and Rutter, N.W., 2002, Differential response of vegetation to postglacial climate in the Lower Salmon River Canyon, Idaho: Paleogeography, Paleoclimatology, Paleoecology, v. 185, p. 339-354.

Deaton, B.C., and Balsam, W.L., 1991, Visible spectroscopy-A rapid method for determining hematite and goethite concentration in geologic materials: Journal of Sedimentary Petrology, v. 61, p. 628-632.

Follmer, L.R., 1996, Loess studies in Central United States: evolution of concepts: Engineering Geology, v. 45, p. 287-304.

Forman, S.L., and Pierson, J., 2002, Late Pleistocene luminescence chronology of the loess deposition in the Missouri and Mississippi river valleys, United States: Paleogeography, Paleoclimatology, Paleoecology, v. 186, p. 25-46.

Grimley, D.A., Follmer, L.R., and McKay, E.D., 1998, Magnetic Susceptibility and Mineral Zonations Controlled by Provenance in Loess along the Illinois and Central Mississippi River Valleys: Quaternary Research, v. 49, p. 24-36.

Grimley, D.A., Follmer, L.R., Hughes, R.E., and Solheid, P.A., 2003, Modern, Sangamon, and Yarmouth soil development in loess of unglaciated southwestern Illinois: Quaternary Science Reviews, v. 22, p. 225-244.

Hall, R.D., and Anderson, A.K., 2000, Comparative soil development of Quaternary paleosols of the central United States: Paleogeography, Paleoclimatology, Paleoecology, v. 158, p. 109-145.

Heslop, D., Langereis, C.G., and Dekkers, M.J., 2000, A new astronomical timescale for the loess deposits of Northern China: Earth and Planetary Science Letters, v. 184, p. 125-139.

Jacobs, P.M., 1998a, Influence of Parent Material Grain Size on Genesis of the Sangamon Geosol in South-Central Indiana: Quaternary International, v. 51/52, p. 127-132.

Jacobs, P.M., 1998b, Morphology and Weathering Trends of the Sangamon Soil Complex in South-Central Indiana in Relation to Paleodrainage: Quaternary Research, v. 50, p. 221-229.

Ji, J., Balsam, W.L., Chen, J., 2001, Mineralogic and Climatic Interpretations of the Luochan Loess Section (China) Based on Diffuse Reflectance Spectrophotometry: Quaternary Research, v. 56, p. 23-30.

Ji, J., Balsam, W.L., Chen, J., and Liu, L., 2002, Rapid and Quantitative Measurement of Hematite and Goethite in the Chinese Loess-Paleosol Sequence by Diffuse Reflectance Spectroscopy: Clay and Clay Minerals, v. 50, p. 210-218.

Ji, J., Chen, J., Balsam, W.L., Lu, H., Sun, Y., and Xu, H., 2004, High resolution hematite/goethite records from Chinese loess sequences for the last glacial-interglacial cycle: Rapid climatic response of the East Asian Monsoon to the tropical Pacific: Geophysical Research Letters, v. 31, L03207.

Johnsen, S.J., Clausen, H.B., Dansgaard, W., Gundestrup, N.S., Hammer, C.U., and Tauber, H., 1995, The Eem Stable Isotope Record along the GRIP Ice Core and Its Interpretation: Quaternary Research, v. 43, p. 117-124.

Kemp, R.A., 2001, Pedogenic modification of loess: significance for palaeoclimatic reconstructions: Earth-Science Reviews, v. 54, p.145-156.

Kim, J.O., and Mueller, C.W., 1978, Introduction to Factor Analysis, Beverly Hills, Sage Publications, 79 p.

Kukla, G., 1987, Loess Stratigraphy in central China: Quaternary Science Reviews, v. 6, p. 191-207.

Kukla, G. and An, Z., 1989, Loess Stratigraphy in Central China: Palaeogeography, Palaeoclimatology, Palaeoecology, v. 72, p. 203-225.

Langmuir, D., 1997, Aqueous Environmental Geochemistry, Upper Saddle River, Prentice-Hall, 600 p.

Leigh, D.S., and Knox, J.C., 1993, AMS Radiocarbon Age of the Upper Mississippi Valley Roxana Silt: Quaternary Research, v. 39, p. 282-289.

Liu, T., and Ding, Z., 1998, Chinese Loess and Paleomonsoon: Annual Review of Earth and Planetary Sciences, v. 26, p. 111-145.

Lowe, J.J., and Walker, M.J.C., 1997, Reconstructing Quaternary Environments, Essex, Pearson Education Limited, 446 p.

Maat, P.B., and Johnson, W.C., 1996, Thermoluminescence and new ^{14}C age estimates for late Quaternary loesses in southwestern Nebraska: Geomorphology, v. 17, p. 115-128.

Maher, B., MengYu, H., Roberts, H.M., and Wintle, A.G., 2003, Holocene loess accumulation and soil development at the western edge of the Chinese Loess Plateau: implications for magnetic proxies of paleorainfall: Quaternary Science Reviews, v. 22, p. 445-451.

Markewich, H.W., Wysocki, D.A., Pavich, M.J., Rutledge, E.M., Millard, H.T. Jr., Rich, F.J., Maat, P.B., Rubin, M., and McGeehin, J.P., 1998, Paleopedology plus TL, ^{10}Be, and ^{14}C Dating as tools in Stratigraphic and Paleoclimatic Investigations, Mississippi River Valley, USA: Quaternary International, v. 51/52, p. 143-167.

Mason, J.A., 1998, Relative Rates of Peoria Loess Accumulation and Pedogenic Processes: Implications for Paleoclimatic Inference: Quaternary International, v. 51/52, p. 169-174.

Mason, J.A., 2001, Transport Direction of Peoria Loess in Nebraska and Implications for Loess Sources on the Central Great Plains: Quaternary Research, v. 56, p. 79-86.

Mason, J.A., Nater, E.A., and Hobbs, H.C., 1994, Transport Direction of Wisconsinan Loess in Southeastern Minnesota: Quaternary Research, v. 41, p. 44-51.

May, D.W., and Holen, S.R., 1993, Radiocarbon Ages of Soils and Charcoal in Late Wisconsinan Loess, South-Central Nebraska: Quaternary Research, v. 39, p. 55-58.

Mirecki, J.E., and Miller, B.B., 1994, Aminostratigraphic Correlation and Geochronology of Two Quaternary Loess Localities, Central Mississippi Valley: Quaternary Research, v. 41, p. 289-297.

Muhs, D.R., and Bettis, E.A. III, 2000, Geochemical Variations in Peoria Loess of Western Iowa Indicate Paleowinds of Midcontinental North America during the Last Glaciation: Quaternary Research, v. 53, p. 49-61.

Muhs, D.R., Ager, T.A., Bettis, E.A. III, McGeehin, J., Been, J.M., Beget, J.E., Pavich, M.J., Stafford, T.W. Jr., Stevens, D.A.S.P., 2003, Stratigraphy and paleoclimatic significance of Late Quaternary loess-paleosol sequences of the Last Interglacial-Glacial cycle in central Alaska: Quaternary Science Reviews, v. 22, p. 1947-1986.

O'Geen, A.T. and Busacca, A.J., 2001, Faunal burrows as indicators of paleo-vegetation in eastern Washington, USA: Paleogeography, Paleoclimatology, Paleoecology, v. 169, p. 23-27.

Porter, S.C., 2001, Chinese loess record of monsoon climate during the last glacial-interglacial cycle: Earth-Science Reviews, v. 54, p. 115-128.

Pye, K., 1995a, The Nature, Origin and Accumulation of Loess: Quaternary International, v. 14, p. 653-667.

Pye, K., Winspear, N.R., and Zhou, L.P., 1995b, Thermoluminescence ages of loess and associated sediments in central Nebraska, USA: Paleogeography, Paleoclimatology, Paleoecology, v. 118, p. 73-87.

Reading, H.G., 1996, Sedimentary Environments: Processes, Facies, and Stratigraphy 3rd ed.: Oxford, Blackwell Science Ltd, 688 p.

Roberts, H.M., Muhs, D.R., Wintle, A.G., Duller, G., A.T., and Bettis, E.A. III, 2003, Unprecedented last-glacial mass accumulation rates determined by luminescence dating of loess from western Nebraska: Quaternary Research, v. 59, p. 411-419.

Rousseau, D.D., and Kukla, G., 1994, Late Pleistocene Climate Record in the Eustis Loess Section, Nebraska, Based on Land Snail Assemblages and Magnetic Susceptibility: Quaternary Research, v. 42, p. 176-187.

Rutledge, E.M., Guccione, M.J., Markewich, H.W., Wysocki, D.A., and Ward, L.B., 1996, Loess Stratigraphy of the Lower Mississippi Valley: Engineering Geology, v. 45, p. 167-183.

Rutter, N.W., Velichko, A.A., Dlussky, K.G., Morozova, T.D., Little, E.C., Nechaev, V.P., Evans, M.E., 2006, New insights on the loess/paleosol Quaternary stratigraphy from key sections in the U.S. Midwest: Catena, v. 67, p. 15-34.

Scwwertmann, U., 1971, Transformation of Hematite to Goethite in Soils: Nature, v. 232, p. 624-625.
Smalley, I.J., Jefferson, I.F., Dijkstra, T.A., and Derbyshire, E., 2001, Some major events in the development of the scientific study of loess: Earth-Science Reviews, v. 54, p. 5-18.

Sun, J., 2002, Provenance of loess material and formation of loess deposits on the Chinese Loess Plateau: Earth and Planetary Science Letters, v. 203, p. 845-859.

Torrent, J., and Barron, V., 2003, The Visible Diffuse Reflectance Spectrum in Relation to the Color and Crystal Properties of Hematite: Clay and Clay Minerals, v. 51, no. 3, p. 309-317.

Wang, H., Mason, J.A., and Balsam, W.L., 2006, The importance of both geological and pedological processes in the control of grain size and sedimentation rates in the Peoria Loess: Geoderma, v. 136, 388-400.

BIOGRAPHICAL INFORMATION

After finishing an undergraduate degree in Geology at Bowling Green State University James signed on with InTEC of DFW as a project geologist in soil engineering. He later moved on to working in the environmental field identifying asbestos minerals through polarized light microscopy and transmission electron microscopy. Amidst a layoff from the environmental industry he started graduate work in geology at the University of Texas at Arlington with renowned researcher Dr. Bill Balsam. Later on during his graduate career he joined with Steve Moody Micro Services, out of financial necessity, again doing asbestos mineral identification through transmission electron microscopy. Currently he plans on accepting an offer with Chesapeake Energy in Oklahoma City, OK to work as an Associate Geologist.